Rafael Rodrigues de Souza

A procedure for the size, shape and topology optimization of transmission line towers

Brazil
2016

Rafael Rodrigues de Souza

A procedure for the size, shape and topology optimization of transmission line towers

Master's Thesis presented as a partial requirement for obtaining a Master's degree in Civil Engineering from the Federal University of Santa Catarina

Federal University of Santa Catarina
Department of Civil Engineering
Graduation Program in Civil Engineering
Advisor: Prof. Dr. Leandro Fleck Fadel Miguel
Co-advisor: Prof. Dr. Rafael Holdorf Lopez

Brazil
2016

Ficha de identificação da obra elaborada pelo autor,
através do Programa de Geração Automática da Biblioteca Universitária da UFSC.

Souza, Rafael
A procedure for the size, shape and topology optimization of transmission line towers / Rafael Souza ; orientador, Leandro Miguel ; coorientador, Rafael Lopez.
Florianópolis, SC, 2016.
133 p.

Dissertação (mestrado) - Universidade Federal de Santa Catarina, Centro Tecnológico. Programa de Pós-Graduação em Engenharia Civil.

Inclui referências

1. Engenharia Civil. 2. Otimização estrutural. 3. Torres de linha de transmissão. 4. Aplicação industrial. 5. Backtracking Search Algorithm. I. Miguel, Leandro. II. Lopez, Rafael . III. Universidade Federal de Santa Catarina. Programa de Pós-Graduação em Engenharia Civil. IV. Título.

Rafael Rodrigues de Souza

A procedure for the size, shape and topology optimization of transmission line towers

Esta Dissertação foi julgada adequada para obtenção do Título de "Mestre", e aprovada em sua forma final pelo Programa de Pós-graduação em Engenharia Civil

Florianópolis, 16 de Agosto de 2016:

Prof. Dr. Glicério Trichês
Coordenador do Curso

Prof. Dr. Leandro Fleck Fadel Miguel
Orientador

Banca Examinadora:

Prof. Dr. Wellison José de Santana Gomes
Universidade Federal de Santa Catarina

Prof. Dr. Otávio Augusto Alves da Silveira
Universidade Federal de Santa Catarina

Prof. Pedro Colmar G. da Silva Vellasco, PhD.
Universidade Estadual do Rio de Janeiro

Acknowledgments

Agradeço aos Professores Leandro Fleck Fadel Miguel e Rafael Holdorf Lopez pelas constantes orientações e lições para a vida.

Deixo também meus agradecimentos a todos Aqueles que de alguma maneira influenciaram minha trajetória, em especial à minha família.

Abstract

This study presents a methodology for topology optimization of transmission line towers. In this approach, the structure is divided in main modules, which can assume different pre-established topologies (templates). A general rule for the templates creation is also presented, which is based in terms of the design practice and feasibility of prototype testing. Thus, these allow that the optimal solution has an important characteristic of direct industrial application. Furthermore, during the optimization process the size and shape of the structure are optimized simultaneously to the topology choice. For numerical examples, two structures were assessed. The first one is a single circuit, self-supported 115 kV transmission line tower. The structure was subjected to a cable conductor rupture scenario and a wind load hypothesis. The second one is a heavier single circuit, self-supported 230kV transmission line tower. The structure was subjected to four different load cases. In both examples the constraints from the ASCE 10-97 code were applied. Due to the non-convex nature of the problem and to the presence of discrete variables in the procedure, the optimization was conducted through the Backtracking Search Algorithm (BSA), which is a modern heuristic algorithm. The results for the size, size and shape, and size, shape and topology optimization are presented and discussed. It is shown that the proposed scheme is able to reduce up to 12% of the structural weight, when compared to a classical size optimization procedure on original structures.

Key-words: Structural optimization. Transmission line towers. Industrial application. Backtracking Search Algorithm.

Resumo expandido

Torres de linha de transmissão (TLT) desempenham um papel significativo no sistema de transmissão. Seu propósito é suspender os cabos condutores e de para-raio, a fim de garantir distâncias elétricas mínimas. As TLT são em geral estruturas treliçadas construídas com perfis do tipo cantoneira. Uma vez que qualquer interrupção no sistema de transmissão gera perdas financeiras significativas, a TLT deve ser projetada respeitando níveis mínimos de confiabilidade, determinados por códigos normativos (IEC (2003), por exemplo).

Devido ao seu potencial, o Brasil é um dos líderes em produção de energia hidroelétrica no mundo. De acordo com a ANEEL (Agência Nacional de Energia Elétrica) mais de 60% da eletricidade consumida no país é de origem hidráulica. Entretanto, a maior parte do potencial hidroelétrico se localiza a milhares de quilômetros dos centros consumidores. Portanto, o Brasil possui uma capacidade instalada similar a Países Europeus, mas com uma rede de transmissão muito maior. Fica clara a importância das linhas de transmissão e consequentemente das torres. Cabe ainda destacar que em uma linha, grande parte das torres são repetidas. Logo, uma redução de custo em uma estrutura será multiplicada pelas suas repetições.

Em um cenário realístico, é esperado que um processo de otimização leve a uma redução de cerca de 10% de massa. Considerando uma torre de 4 toneladas com ocorrência media de 2,5 TLT/km, isso representaria uma economia de 1 ton/km de LT. Utilizando o preço do aço laminado, estimado em 2015 em torno de R$ 5,00/kg, em uma LT curta de 300 km, a economia seria de R$ 1.500.000. Em uma LT longa, com 1.000 km, a economia chegaria a R$ 5.000.000.

Alguns estudos, focando em exemplos acadêmicos, tem sido realizados no contexto de otimização de torres treliçadas. Rajan (1995), Natarajan &

Santhakumar (1995), Gomes & Beck (2013),Taniwaki & Ohkubo (2004), Sivakumar *et al.* (2004), Mathakari *et al.* (2007), Kaveh, Gholipour & Rahami (2008), Noilublao & Bureerat (2011).

Embora estes estudos tenham apresentado diversos avanços, alguns aspectos adicionais devem ser levados em consideração, quando se busca uma aplicação industrial direta da estrutura otimizada. Um dos principais aspectos não abordados nestes trabalhos, está relacionado a viabilidade construtiva da estrutura final e seu desempenho em ensaio de protótipo.

Por outro lado, alguns estudos têm abordado uma aplicação industrial direta, considerando em algum nível tais aspectos. Por exemplo, Shea & Smith (2006), Parıs *et al.* (2010), Guo & Li (2011), Parıs *et al.* (2012), Chen, Yuan & Jiang (2014),

Estes estudos adotam basicamente estratégias de modificação *localizadas* a fim de atualizar a topologia da estrutura. Note que o termo *localizada* é empregado para mostrar que as variações permitidas são a nível de nós e elementos, os quais podem ser criados ou removidos e movimentados dentro de certos intervalos (i.e., pequenas partes da estrutura são modificadas). Entretanto, conduzir modificações através dos nós e elementos diretamente pode levar a certas desvantagens. A solução final pode não ser melhorada significativamente se comparada com otimização dimensional e geométrica (Shea & Smith (2006)), pode ser inviável do ponto de vista construtivo (Shea & Smith (2006)) e apenas algumas partes da estrutura podem ser otimizadas eficientemente (Guo & Li (2011), Chen, Yuan & Jiang (2014)). Além disso, se torna difícil avaliar corretamente os comprimentos de flambagem quando barras são removidas da estrutura Torii, Lopez & Biondini (2012).

É possível ainda observar que em todos os trabalhos mencionados anteri-

ormente, foi imposta simetria nas quatro faces da estrutura. Entretanto, esta característica não é sempre adotada nos projetos de TLT. O treliçamento defasado, o qual possui uma configuração simétrica apenas em duas faces, é de fato uma solução usual para torres convencionais de médio porte (com altura média em torno de 50 metros). Destaca-se ainda que estas torres representam a maior parte das estruturas em uma linha de transmissão usual.

Logo, o principal objetivo deste trabalho é propor uma metodologia para otimização topológica de torres de linha transmissão, focando em uma aplicação industrial. Em contraste com estudos anteriores, os quais se baseiam em modificações *localizadas* da topologia, a metodologia proposta adota uma estratégia global de modificações. Nesta, a estrutura da torre é dividida em módulos principais compostos por um grande conjunto de elementos estruturais. Estes módulos principais são entidades globais as quais podem assumir diferentes topologias pré-estabelecidas (*templates*). Estes *templates* são concebidos a fim de garantir a viabilidade construtiva e de testes de protótipo. Consequentemente, a metodologia de otimização incorpora restrições de códigos normativos (como por exemplo aquelas relacionadas a esforços, deslocamentos, índices de esbeltez) bem como a viabilidade construtiva e de teste de protótipo. Permitindo que a metodologia possua um caráter de aplicação industrial direta.

Como demonstrado experimentalmente por CIGRÉ (2009) a topologia desempenha um papel importante no comportamento estrutural de torres observado em testes de protótipo. Mesmo pequenas variações na configuração (como por exemplo no padrão de treliçamento ou na posição dos diafragmas) afeta diretamente o comportamento da estrutura e a compatibilidade com o modelo mecânico adotado. Estes e outros aspectos de grande significância prática podem ser considerados na construção dos *templates* disponibilizados para o processo de otimização. Dessa forma, a regra de criação de *templates* é apresentada e explicada no corpo do texto.

Finalmente, outra vantagem importante desta metodologia é que o espaço de busca é limitado para que apenas as topologias mais comuns empregadas na industria possam ser disponibilizada como *templates*. De fato, a ideia de reduzir o espaço de busca tem sido empregada por outros pesquisadores, Como exemplo, Shea & Smith (2006) e Guo & Li (2011) reduziram o espaço de busca em suas propostas de otimização topológica. Logo, entre os objetivos deste estudo está manter as vantagens de limitar o espaço de busca (a fim de cumprir requisitos construtivos e reduzir os custos computacionais), além de introduzir o conceito de otimização baseada em *templates*.

Devido à característica não-convexa da função objetivo, bem como à presença de variáveis discretas, o algoritmo heurístico BSA (*Backtracking Search Algorithm*) foi empregado. Este algoritmo foi desenvolvido por Civicioglu (2013), e tem mostrado resultados promissores para otimização topológica de estruturas treliçadas, conforme pode ser visto em Souza *et al.* (2016).

A metodologia proposta é testada em dois exemplos de torres comumente encontradas na indústria Brasileira. No primeiro, uma torre autoportante de circuito simples de 115kV, submetida a dois casos de carregamento, é otimizada. A otimização dimensional atingiu como melhor resultado 1950,5 kg, mas ao incorporar a otimização geométrica o resultado encontrado foi de 1880,4 kg. Por fim, a metodologia proposta para otimização topológica foi implementada, levando a uma massa de 1809,8 kg, que representa uma redução de 7,22% em relação à otimização apenas dimensional.

O segundo exemplo consiste em uma torre autoportante de circuito simples de 230kV, submetida a quatro casos de carregamento. Para este exemplo, a otimização dimensional atingiu uma massa de 2324,7 kg, enquanto a otimização dimensional e geométrica levou a um resultado

de 2138,1 kg. Ao incorporar a metodologia proposta de otimização topológica, o resultado atingido foi de 2041,7 kg, que representa uma redução de 12.2% na massa da estrutura, quando comparada com à otimização apenas dimensional.

Os resultados obtidos mostram que a metodologia proposta é bastante promissora e que esforços adicionais são ainda necessários. Outros exemplos devem ser estudados, de modo que a proposta de otimização baseada em *templates* possa abranger diferentes tipos torres de transmissão, inclusive torres estaiadas.

Palavras-chaves: Otimização estrutural. Torres de linha de transmissão. Aplicação industrial. *Backtracking Search Algorithm.*

List of Figures

List of Tables

List of abbreviations and acronyms

TL	Transmission line
TLT	Transmission line tower
ANEEL	Brazilian National Agency of Electrical Energy - *Agência Nacional de Energia Elétrica Brasileira*
BSA	Backtracking Search Algorithm
Var.	Shape variation
S.D.	Standard deviation
OFE	Objective function evaluation

List of symbols

V_1	Vertical semi-span
V_2	Vertical semi-span
l_1	Horizontal semi-span
l_2	Horizontal semi-span
$\Re$	Real domain
W	Structural weight
ρ	Specific mass
l	Length
$\mathbf{x}$	Variable vector
P	Initial population of BSA
P_{pert}	Perturbed population of BSA
t_{top}	Size of the population
n_v	Dimension of the problem
P_{hist}	Historical population
$\mathbf{M}$	Mixrate matrix
L_{xx}	Buckling length in the x-axis
L_{yy}	Buckling length in the y-axis
L_{zz}	Buckling length in the z-axis
r_{xx}	Radius of gyration in the x-axis
r_{yy}	Radius of gyration in the y-axis

r_{zz}	Radius of gyration in the x-axis
a_i	Size variables
ξ_i	Shape variables
τ_i	Topology variables
σ	Axial stress
λ	Slenderness ratio
w	Flat width of the angle profile
t	Thickness of the angle profile
m_r	Mixrate parameter
C	Number of cycles
$t.b.$	Tower body
α	Tower slope
θ	Angle between diagonals
$i.e.$	Length of inferior edge
$s.e.$	Length of superior edge
S_d	Design load
R_d	Design resistance
R_n	Nominal resistance
F_a	Compressive stress
ϕ_r	Stress factor
F_y	Minimum guaranteed Yield stress
E	Modulus of elasticity

K	Effective length coefficient
F_{cr}	Compressive stress for angle members
F_t	Tension stress

Summary

1 Introduction

1.1 Motivation

Overhead transmission lines (TL) are designed to transport electrical energy from a power plant to an electrical substation (Figure 1). In general, the generating stations (hydroelectric, thermoelectric or nuclear, for instance) are located at large distances from the consuming center. Therefore, the electricity is transmitted at high voltages (115 kV or higher) in order to reduce the energy loss due to the long transmission distance. In a country with continental dimensions such as Brazil, it is not rare TLs with more than a thousand kilometers.

Figure 1 – Transmission line

Source: www.mpomontagens.com.br/servicos/projetos/linhas-de-transmissao/

The transmission line towers (TLT) play an important role in the TL system. They are generally latticed structures formed by steel angle sections with the purpose to suspend cable conductors and ground wires to guarantee the minimum electrical clearances required. Because any interruption in the system causes severe economic losses, the TLT must

be designed to attain the reliability levels determined by the codes (IEC (2003), for instance). Moreover, a fail in any component will interrupt the overall transmission capacity, since a TL is a series system.

Despite this apparent simple configuration, TLT structures are widely regarded as one of the most difficult lattice structures to analyze. This difficulty stems from the fact that these structures are generally composed of asymmetric thin-walled angle section members eccentrically connected. For this reason proof-loading or full-scale testing of the structure has traditionally formed an integral part of the development of tower design. Stress calculations in the structure are normally obtained from a linear elastic analysis where members are assumed to be axially loaded and, for the majority of cases, pin-connected. In practice, such conditions do not exist and members are detailed to minimize bending stresses Al-Bermani & Kitipornchai (1993).

Due to these reasons, several efforts have been conducted to better understand the structural behavior of TLT, for example Al-Bermani & Kitipornchai (1993), Kitipornchai, Al-Bermani & Peyrot (1994), Zhu, Al-Bermani & Kitipornchai (1994). Considering the Brazilian researchers, TLTs has been studied by Loredo-Souza & Davenport (1998), Loredo-Souza & Davenport (2001), Loredo-Souza & Davenport (2003), Oliveira *et al.* (2003), Oliveira *et al.* (2006), Battista & Pfeil (2009), Carvalho (2010), Miguel *et al.* (2012), Mara (2013), Carvalho (2015), Miguel *et al.* (2016) with main focus on the effects caused by the wind loads. Gontijo (1994), Vellasco *et al.* (2002), Silva *et al.* (2003), Gabrielli (2004), Oliveira *et al.* (2007), Kaminski-Jr. *et al.* (2008), Singh (2009), Rabelo, Jr & Greco (2014), Costa (2014), discussed structural models currently adopted in TLTs, as well as the behavior and design of these structures. Azevedo (2007), Azevedo & Diniz (2008), Azevedo (2011), Azevedo & Diniz (2012) evaluated the reliability levels of TLTs foundations. It can be cited the contributions of Rodrigues, Battista & Pfeil (2001), Battista, Rodrigues & Pfeil (2003), Rodrigues, Battista & Pfeil (2004), Rippel (2005), Rodrigues, Battista & Pfeil (2005), Argenta (2007) assessing the dynamic behavior of TLTs. Finally, Neto (2012) and Conceição (2013)

studied the downbursts effects on TLTs.

In spite of the reasonable amount of investigations, optimization studies on TLTs are still incipient. In contrast to some structures that are generally unique (e.g. bridges and buildings), the same design of a given transmission line tower is frequently built several times, up to hundreds of times in a single transmission line. Thus, cost savings and performance improvements obtained by structural optimization procedures can have a large impact in the entire system.

According to Al-Bermani & Kitipornchai (1993), any saving in the design of one tower is magnified many times over because large numbers of towers of the same designs are usually constructed. For example, in a 250 km transmission line, there may be 500 towers of which up to 80% are of the same type. Furthermore, according to Fang, Roy & Kramer (1999), TLTs usually accounts for 30 to 40% of the total cost of a TL. Therefore, selecting an optimum structure becomes an integral part of a cost-effective transmission line design.

In a realistic scenario, it would be expected that an optimization procedure could lead to around 10% of saving costs. Then, if one considers a 4 ton tower with an average occurrence of 2.5 TLT/km, this would represent an economy of 1 ton/km of TL. Taking into account the price of the laminated steel, estimated in 2015, around R$ 5.00/kg, in a short length TL with 300 km, the saving costs could reach up to R$ 1,500,000. In a large length TL, with 1,000 km, the savings would be R$ 5,000,000.

1.2 Literature review

The structural optimization of trusses has been widely studied (Dorn (1964), Sved & Ginos (1968), Dobbs & Felton (1969), Pedersen (1972), Hemp (1973), Goldberg & Samtani (1986),Rajeev & Krishnamoorthy (1992), Camp & Farshchin (2014), Wu & Chow (1995), Galante (1996), Tang, Tong & Gu (2005), Kelesoglu (2007), Grierson & Pak (1993), Rajan (1995), Hajela & Lee (1995), Rahami, Kaveh & Gholipour

(2008), Torii, Lopez & Biondini (2012), Miguel, Lopez & Miguel (2013b), Wang & Ohmori (2013), Torii, Lopez & Miguel (2014)).

Methods for the size optimization of truss structures, in which the member areas are taken as design variables, are fully established in the literature (Hemp (1973),Pedersen (1972),Adeli & Kamal (1991)). However, it is well-known that better results can be achieved when size, shape, and topology optimization are performed simultaneously Dominguez, Stiharu & Sedaghati (2006). In this case, the problem generally begins with a ground structure to determine the best element topology, and truss geometry can also be altered by taking nodal coordinates as design variables Saka (1980). Figure 2 illustrates the different truss optimization level types.

Figure 2 – Truss optimization level types

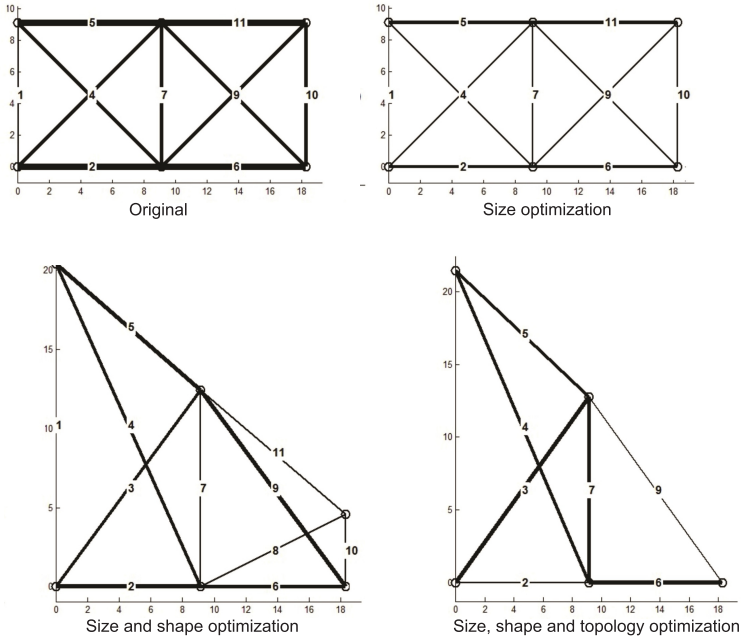

Some studies, focusing on academic research, have already been performed in the context of optimization of truss towers. Rajan (1995) presents a method to optimize the size and shape of a transmission tower submitted to multiple load cases. Natarajan & Santhakumar (1995) studied the reliability based optimization of a truss tower submitted to multiple load cases under stress constraints. Gomes & Beck (2013) studied the size and shape optimization of a plane truss tower considering loads and material properties uncertainties, and a wind load that varies with the strain process.

Taniwaki & Ohkubo (2004) studied the optimization of size, shape and Young's modulus of an 88.2 meters high tower. The structure is evaluated as plane truss, under stress, displacement and slenderness ratio constraints. Sivakumar *et al.* (2004) present a discrete size optimization of a truss tower under constraints that follows the Indian code.

Mathakari *et al.* (2007) present a reliability based method for the size, shape and topology optimization of a truss tower. The size optimization is performed considering discrete values and the topology optimization is employed by layers, where the number of layers and the distance between each layer and the base are taken as design variables. During the optimization, the structure is submitted to a variable wind load and is evaluated according to displacements and stresses, determined according to the recommendations from AISC (2001).

Kaveh, Gholipour & Rahami (2008) studied a structure submitted to two load cases, considering continuous values of cross sectional areas for the size optimization. The structure is evaluated under stress and slenderness ration constraints, determined following the ASCE 10-15 (2015) and maximum displacements in specific nodes.

Noilublao & Bureerat (2011) studied the size, shape and topology optimization of a truss tower, considering discrete values of cross section area. The structure is submitted to multiple load cases, while is evaluated under stress and slenderness ratio constraints. On this study the topological optimization employs a layer approach, similar to Mathakari *et al.* (2007). However, after the variation of the number of layers it is

possible that the members assume null values of cross-sectional area.

Although these studies presented several advances, some important additional aspects must be taken into account for a direct industrial application concerning the optimal design of transmission line tower structures. One of the main issues not addressed in the previously mentioned papers is related to constructive feasibility of the design and its performance in prototype testing.

On the other hand, some works addressing direct industrial applications, which take into account such aspects to some degree, can also be found in literature. Shea & Smith (2006) addressed optimization of a full-scale transmission line tower. The structure is subjected to multiple load cases and code constraints. However, the optimal structural designs obtained do not agree with regular configurations normally acceptable for a construction and prototype testing. Besides, the procedure imposes the design to be symmetric in its four faces, which is not always used in transmission towers.

Parıs *et al.* (2010) studied the shape optimization of a transmission line tower, subjected to multiple load cases and code constraints. Because the procedure is based on continuous design variables, it is not able to ensure that the final design is composed by commercially available profiles.

Guo & Li (2011) performed the size, shape and topology optimization of a large-scale transmission line tower. The structure is subjected to one wind load case and code constraints. The topology optimization is performed in the inclined part of the tower body (below its waist) using two different methods. In both cases the optimal design is necessarily symmetric in the four faces of the tower.

Parıs *et al.* (2012) performed the size and shape optimization of a transmission line tower subjected to multiple load cases considering discrete values of cross-sectional areas and code constraints. The optimization was performed by dividing the structure into blocks. Since the geometry of the blocks is changed independently, the final design presents differences between the slopes of the legs in each block. This

makes the final design unfeasible from the constructive and prototype testing points of view. Additionally, the optimization procedure also imposes symmetry in the four faces of the design.

Chen, Yuan & Jiang (2014) presented an approach where the tower body shape is selected first and then the components' types are optimized. The procedure considers discrete values of cross-sectional areas. In the process of tower body shape modification, the number of tower sections, the height of each section, and the type of diaphragm used are changed, considering stress and stability constraints. As in previous studies, symmetry on all faces is imposed.

1.3 Scope and objective of the study

The previously mentioned literature basically adopts *localized* modifications strategies to update the structural topology. Note that the term *localized* is employed here to refer that the allowable changes are in the level of nodes and elements, which can be created or removed, and moved within certain intervals (i.e., small parts of the structure are modified). However, carrying out modifications to nodes and elements directly can lead to some other important drawbacks. The final design may not be significantly improved in comparison to size and shape optimization (Shea & Smith (2006)), it can be unfeasible from the constructive point of view (Shea & Smith (2006)), and only some part of the structure may be effectively optimized (Guo & Li (2011), Chen, Yuan & Jiang (2014)). Furthermore, it becomes difficult to correctly evaluate effective buckling lengths when bars are removed from the structure (Torii, Lopez & Biondini (2012)).

Another important observation is that all the previously mentioned studies imposed symmetry to all faces of the structure. However, this approach is not always adopted in the design of full-scale transmission line towers. Staggered bracing, which is a non-symmetric configuration, is indeed a very usual solution in design of conventional towers (with an average height up to 50m), that commonly represent the largest portion

of structures in a given transmission line.

Therefore, the main objective of this work is to propose an approach for topology optimization of transmission line towers focusing on industrial applications. In contrast with previous works, which are based on direct local modifications of the structural topology, the proposed approach adopts a global modification strategy. In this approach, the structure of the tower is divided into main modules composed by a large set of structural elements. These main modules are global entities that can assume different pre-established topologies (templates). These templates are conceived in order to ensure constructive and prototype testing feasibility. Consequently, the optimization approach incorporates standard design constraints (such as those related to stresses, displacements, slenderness ratios) and constructive and prototype testing feasibility. This allows the approach to be employed for direct industrial applications.

Since the problem deals with discrete design variables and the nonconvex characteristic of the objective function, the Backtracking Search Algorithm (BSA) is employed herein. This algorithm was recently developed by Civicioglu (2013), and has shown very promising for topology optimization of truss structures as can be seen in Souza *et al.* (2016).

Specific objectives can be also listed:

- Employ an automatic routine inside the optimization process to determine the wind loads on TLT;
- Develop a general rule for the creation of templates.

1.4 Organization of the text

The thesis is divided in six chapters. This chapter (Chapter 1) aims to introduce and delimit the research scope.

The second chapter (Chapter 2)presents a general explanation of TLTs and their purpose on the electrical system. The structures are

classified according to its characteristics and the typical load cases are illustrated. Finally, a brief description of prototype testing as well as a comprehensive discussion on the structural tower modeling is carried out.

The third chapter (Chapter 3) presents and overview on engineering optimization. The main definitions are presented as well as the classification of the optimization problems. Then, the solution algorithms are explained and their differences are highlighted. Finally, the BSA heuristic algorithm, which is employed in the ensuing analysis, is detailed.

The fourth chapter (Chapter 4) details the proposed templates based approach for topology optimization of TLTs. The stages of the topology optimization are presented and their impact on staggered bracing towers is discussed. Furthermore, a general rule for the templates creation is also introduced. Finally, the optimization formulation of the studied problem is illustrated.

The fifth chapter (Chapter 5) presents two numerical examples. The first one is a single circuit, self-supported 115kV transmission line tower subjected to a cable conductor rupture scenario and a wind load hypothesis. The second one is a heavier single circuit, self-supported 230kV transmission line tower, subjected to four load cases, including wind load hypothesis, construction or maintenance load scenario and cable rupture hypothesis.

Finally, the sixth chapter (Chapter 6) presents the concluding remarks and suggestions for future studies.

2 Transmission line towers

This chapter presents a general explanation of TLTs and their purpose on the electrical system. First, the main features of the tower geometry and its definition process are discussed. Then, the structures are classified according to its characteristics and the typical load cases are illustrated. Finally, a brief description of prototype testing as well as a comprehensive discussion on the structural tower modeling is carried out. For further details on this subject, the reader is referred to Gontijo (1994), Fang, Roy & Kramer (1999), Kaminski-Jr (2007), CIGRÉ (2009) and the references therein.

2.1 General information

An electrical power system is a network (electrical grid) constructed to connect and transport the electricity from the power plants to consumers. It is composed by the generating stations that supply the power, the transmission systems that carry the electricity to demand centers and distribution systems that furnish it to the individual customers. Figure 3 presents a general overview of the electrical system.

Due to its potential, Brazil is one of the leading producers of hydroelectric power in the world. According to the Brazilian National Agency of Electrical Energy (ANEEL) more than 60% of the electricity consumed in the country has a hydraulic origin. However, most of this hydroelectric potential lays thousands of kilometers from the populations centers. Therefore, the Brazilian installed electrical capacity is similar to European countries, but with a much larger transmission network. As a consequence, the constructed TLs present, in great part, a significant length.

Still according to ANEEL, the Brazilian transmission grid has increased almost 40% in less than 15 years. It was around 64,000 km

Figure 3 – Overview of the electrical system

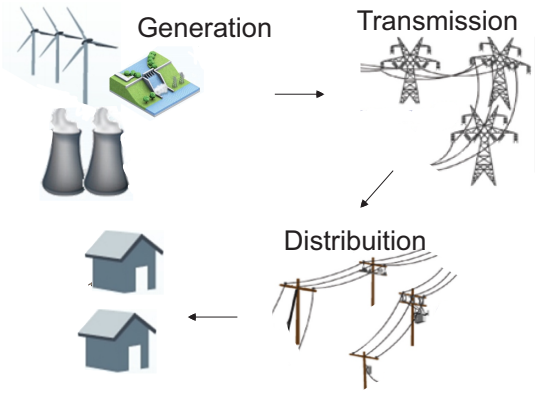

in 1998, passing to 72,000 km in 2002 and reaching almost 100,000 km in 2011. Figure 4 illustrates the current and planned TL above 138kV in Brazil. For these voltages, the latticed steel towers are the most economical solutions for the supports and they are usually employed Gontijo (1994). Two types of transmission structures are shown in Figure 5.

2.2 Tower configuration

The support final configuration is dependent of previous definitions adopted during the electrical TL design. According to Fang, Roy & Kramer (1999), some key factors that influence the structure configuration are:

- A horizontal phase configuration usually results in the lowest structure cost.
- If right-of-way costs are high, or the width of the right-of-way is restricted or the line closely parallels other lines, a vertical configuration may be lower in total cost.

Figure 4 – Existing and future transmision lines in Brazil

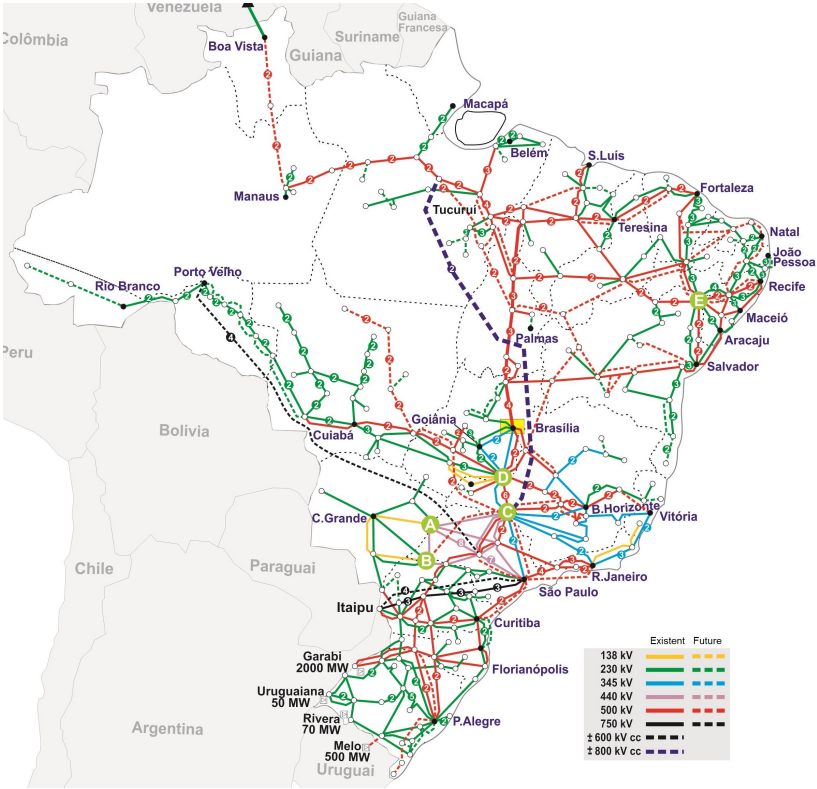

Source: Brazilian Operator of the National Electrical System - *ONS - Operador Nacional do Sistema Elétrico*

Figure 5 – Transmission structure: truss tower (left) and pole (right)

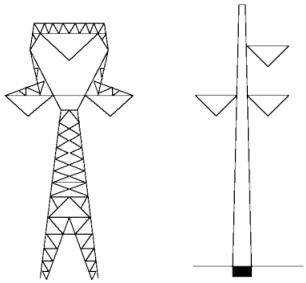

Fonte: Fang, Roy & Kramer (1999)

- In addition to a wider right-of-way, horizontal configurations generally require more tree clearing than vertical configurations.
- Although vertical configurations are narrower than horizontal configurations, they are also taller, which may be objectionable from an aesthetic point of view.
- Where electric and magnetic field strength is a concern, the phase configuration is considered as a means of reducing these fields. In general, vertical configurations will have lower field strengths at the edge of the right-of-way than horizontal configurations, and delta configurations will have the lowest single-circuit field strengths and a double-circuit with reverse or low-reactance phasing will have the lowest possible field strength.

Because the tower structural designer does not interfere in these definitions, only the support geometry and bracing pattern must be determined in this stage. Thus, the engineer must establish dimensions for the tower body (inclined and straight), crossarms, shield wire peak, bracing pattern and the slope of the tower leg. Basically, the final geometry of a TLT is mainly dependent on four factors:

- The tower height is a function of the span length of the conductors between structures;
- The starting point to choose the geometry is the minimum cable conductor to cable conductor and cable conductor to steel clearance requirements, which depend on the line voltage;
- The width of the tower base is a function of the tower leg slope (which is also limited by the cable conductor to steel clearance requirements);
- The height of the tower peak depends on shielding considerations for lightning protection.

The final tower structure is composed of a basic body, body extensions and leg extensions. The basic body is employed for the entire set of towers. On the other hand, the extensions (body and leg) are added to the basic body to reach the pre-established tower height for a specific structure. Figure 6 illustrates these main components. This tower composition is the so-called structure family. The family concept allows avoiding the design to be individually performed. Then, a consequent economy in the global process can be achieved (considering design and fabrication).

There are, in general, at least three types of tower families in a TL: tangent, angle, and deadend structures. The tangent towers are used when the line is straight or has a very small angle, not exceeding 3°. This type of structure usually represents 80% to 90% of the towers on a TL. The angle towers are employed when the line must change its direction. Finally, the deadend tower is used when the line angle exceed 30° or as a terminal tower. In addition to the function in a TL, it is possible to classify the towers in accordance with the following aspects:

Figure 6 – Scheme with the main components of a transmission tower.

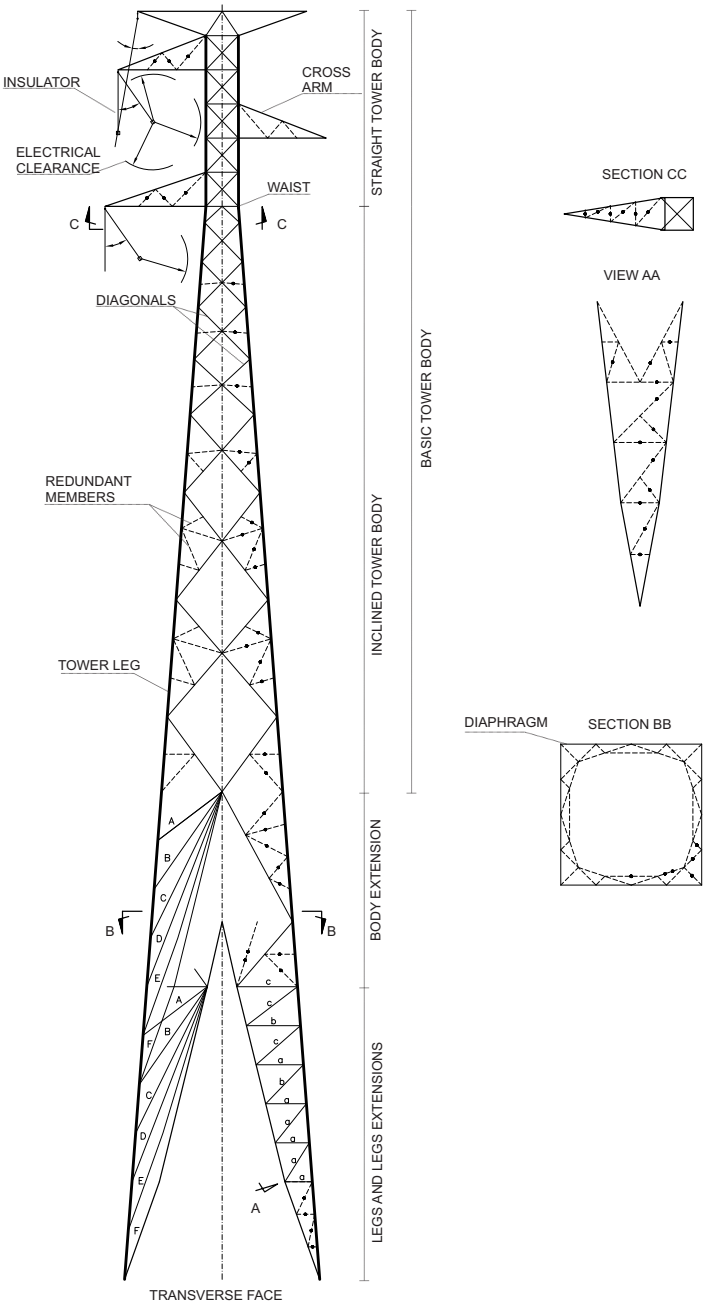

Figure 7 – Examples of the transmission line structures

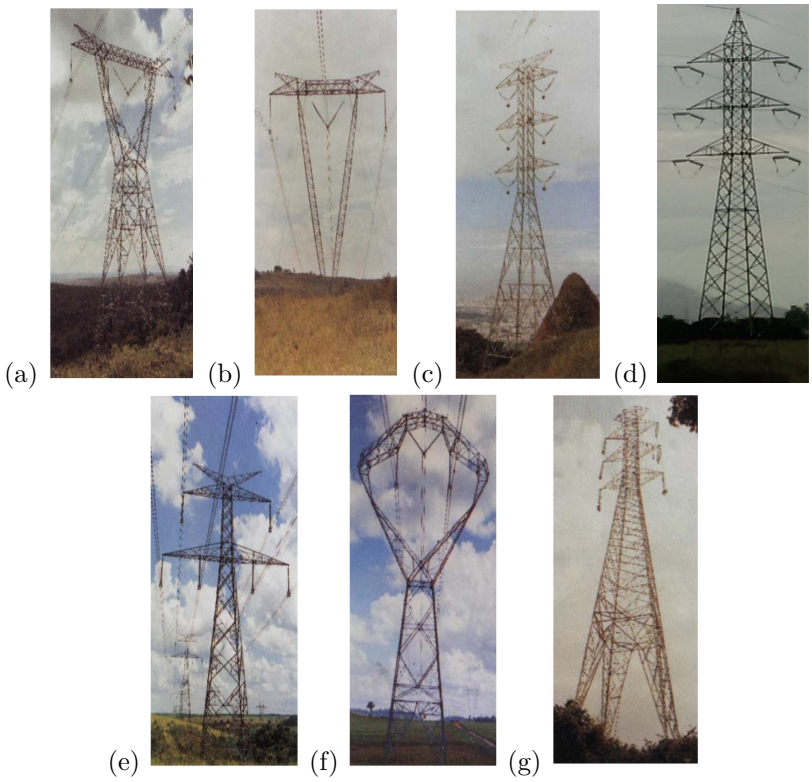

Source: Kaminski-Jr (2007)

- Number of circuits: single and double (Figure 7 (a), (b), (f) and (c), (d), (e), (g), respectively);
- Phase orientation: triangular, horizontal and vertical (Figure 7 (e), (f); (a), (b) and (c), respectively);
- Structural type: self-supported and guyed towers (Figure 7 (a), (c), (d), (e), (f), (g) and (b), respectively);

- Bracing pattern: continuous or staggered (Figure 7 (a), (b), (c), (e), (f), (g) and (d), respectively).

Stress calculations in the structure are normally obtained from a linear elastic analysis where members are assumed to be axially loaded and, for the majority of cases, pin-connected. In practice, such conditions do not exist and members are detailed to minimize bending stresses. Moreover, when a truss type model is used to analyze a transmission tower, the structure should be free of planar joints which cause local instability. Significant effort is required on the part of the designer to remove planar joints, a process which requires the addition of stabilizing members. Identifying and correcting such instabilities may require a few additional computer runs. A structural modeling alternative is to represent the main leg members as continuous beams Al-Bermani & Kitipornchai (1993).

Based on experimental evidence, Kaminski-Jr (2007) has verified that regardless the structural model adopted (3D-truss or 3D-frame elements) the bending stresses are not significant when adopting the usual Brazilian industrial structural configurations and detailing. On the other hand, some specific structural details could greatly influence the bolt slippage in connections. This will be comprehensively discussed in Section 2.5.

2.3 Loads on transmission line towers

The main load cases acting on TLTs are due to self-weight, cable rupture and climate reasons, such as wind and ice. Depending on these origins, they must be applied in the vertical, longitudinal or transversal direction to the TL.

The vertical loads are due to the self-weight of the tower, the cable conductors, the shield wires and the insulators. For tangent towers, the cables' weight must be divided between the two adjacent structures, considering their vertical semispans, as illustrated in Figure 8 as V_1 and V_2. In addition, the most significant load to the crossarms (or shield

wire peaks) occurs during the installation of the cables on the structures (vertical).

The transverse loads are caused by the wind pressure acting on cable conductors, shield wires, insulators and towers. Furthermore, there is a transverse force component from the cables' tension in structures with line angles. The wind load is determined taken into account the wind direction and its pressure (following the code recommendations, for instance, ABNT (1988) or IEC (2003)). According to Kaminski-Jr (2007) the wind loads are responsible for around 80% of the stresses on structural members. Similarly to the cables' weight, the wind loads must be divided between two adjacent towers. However, in this case it should be taken the horizontal semispans (simply the distance between the midpoints of adjacent towers), as shown in Figure 8 as $1/2l_1$ and $1/2l_2$.

Figure 8 – Horizontal and vertical semispans.

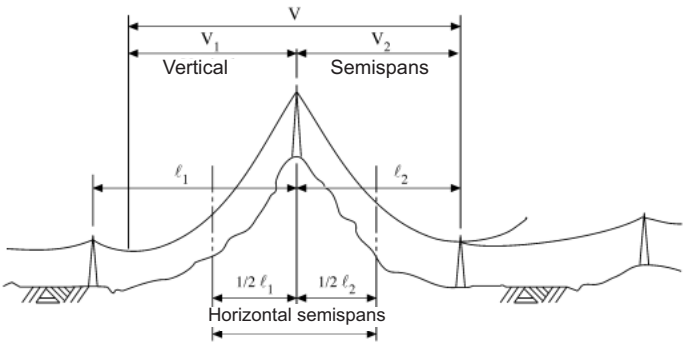

Source: Fang, Roy & Kramer (1999, pg. 3)

The most important longitudinal load is the one caused by a cable rupture hypothesis. The consideration of this load case has an important function of trying to prevent a TL cascading effect (a progressive failure

of structures). Additionally, it is also recommended to install heavy angle or deadend towers occasionally along the TL.

Other important loads occur in deadend towers (longitudinal), angle towers (transversal and longitudinal) when the tension in the cables is different on each adjacent span. Figure 9 presents a scheme of the typical loads acting in transmission towers.

Figure 9 – Typical load cases.

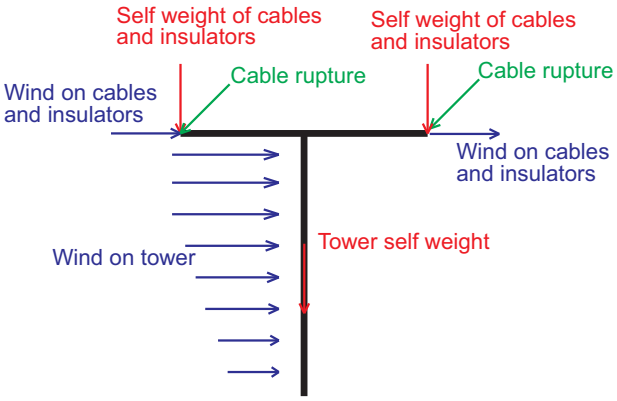

Source: Kaminski-Jr (2007, p. 83)

2.4 Prototype testing

The full scale prototype tests are usually performed for new tower designs (for at least the tangent towers). During these tests the structures must resist to 100% of the ultimate design loads. Therefore, it is possible to prevent that design mistakes would be spread to the industrial production. Moreover, they are able to provide important qualitative information to the tower designer regarding the global structural behavior before failure.

According to Menezes (1988) the prototype tests can be divided in destructive and non-destructive tests. While in the former the rupture of the support is achieved, in the latter the structure is tested until 100% of the design load. Thus, for the non-destructive test, the rupture may or may not be reached. The design loads are applied through a system of cables and pulleys, as shown in Figure 10.

Figure 10 – Prototype test in transmission line towers.

Source: Kaminski-Jr (2007, p. 85)

2.5 Impact of topology on structural behavior of transmission line towers

The current industrial practice for structural design of transmission line steel towers usually adopts linear-elastic (or geometrical non-linear) analysis using 3D-truss or frame elements. Despite the simple model employed, it has been recognized by engineers that some sources of non-linear effects may appear, mainly associated to the actual behavior of the tower connections (Al-Bermani & Kitipornchai (1990), Kitipornchai, Al-Bermani & Peyrot (1994), Kroeker (2000), Ungkurapinan *et al.* (2003), Ahmed (2007), Kaminski-Jr (2007)).

Initial studies (Kitipornchai, Al-Bermani & Peyrot (1994)) focused on assessing the effect of bolt slippage on structural behavior, rather than developing realistic models, due to the lack of reliable experimental data available. The results indicated that the slippage of bolts might have some effects on deflection, but does not significantly influence the ultimate strength of the structures.

One of the first experimental investigations carried out to better understand the structural behavior of transmission line towers was promoted by CIGRÉ (1991). A prototype structure was constructed and some internal member forces were measured. These results showed important discrepancies among the predictions provided by a group of 27 international designers. Moreover, the predictions among the engineers themselves also presented important divergences, due to their distinct modeling assumptions.

A new experiment was proposed by CIGRÉ (2009). Three new prototype structures with small differences in their topologies were constructed and tested. Although these differences were slight, they played an important role in the rigidity of the structures. Despite the discrepancies decreased, they were still present in some diagonals of the two stiffer structures, while in the most flexible prototype the internal forces were coincident.

Then, using the experimental load-slip relationship results of

typical tower angles determined by Ungkurapinan *et al.* (2003), CIGRÉ (2009) modeled the connections of the prototype structures tested as nonlinear springs. The results were compared to the monitored data, showing that the structural prediction of the two stiffer structures approached the experimental observation.

The second CIGRÉ (2009) experimental investigation confirmed what tower design engineers believed, based on their observations of full-scale tower testing: the more the structural stiffness increases, the more the bolt slippage impacts on the tower behavior. In addition, predictions made by simple models are more discrepant in some members as the structural stiffness increases. Because the topology is directly related to the tower stiffness, the structural configuration chosen by the designer has great influence in the degree of convergence between the theoretical predictions and the measured results obtained in the tests.

Thus, it was recommended to designers a careful attention in the topology definition, mainly observing details that could contribute to increase the structural stiffness. In practice, simple aspects as the position of the diaphragms and the diagonals configuration would be enough the make the tower more flexible and, thus, less prone to the bolt slippage effects.

Observe in Figure 11 the differences in the diaphragms position and in the diagonals configuration in Models 1 and 2. The diagonals configuration between the inclined and straight tower bodies as well as the cross-sectional configuration shown in Section M2 provide to the Model 2 a significant increase in its stiffness. Indeed, diagonal edges in "X" configuration provide an increment in tower stiffness. Therefore, it would not be indicated that the transitions between the inclined and the straight tower bodies be done with "X" diagonal in both tower faces. In practice, it is recommended that this transition be similar to the one presented in Model 1. In addition, it is recommended that the diaphragm should be located in the superior part of the extension (as it is shown in Section M1).

Consequently, if the designer takes these premises into account

Figure 11 – Difference on the topology of transmission line towers

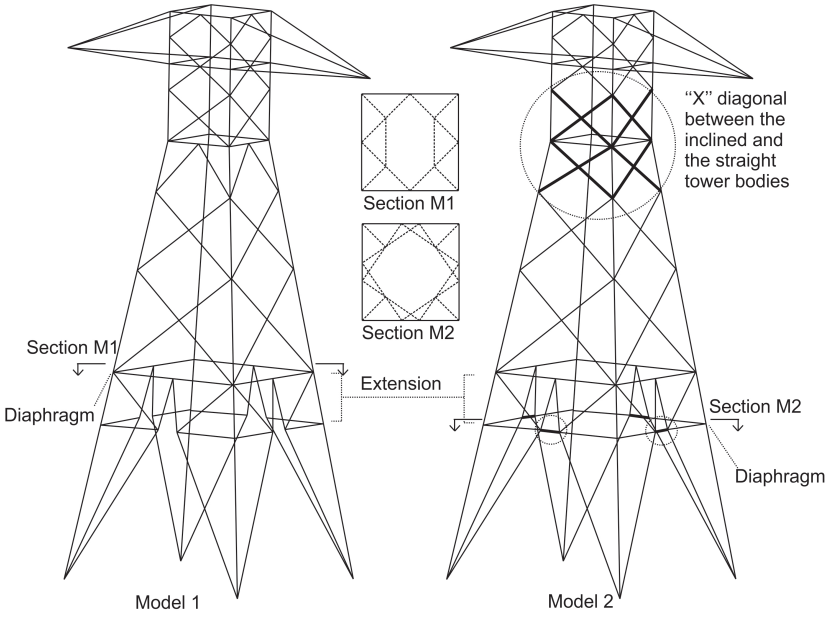

Source: Adapted from CIGRÉ (2009)

in the topology definition, at least in some degree, the theoretical predictions carried out by simple models would be more liable to the actual structural behavior.

3 Optimization

This chapter presents an overview on engineering optimization. Firstly, the main definitions are shown as well as the classification of the optimization problems. Then, the solution algorithms are explained and their differences are highlighted. Finally, the BSA heuristic algorithm, which is employed in the ensuing analysis, is detailed. For further details on this subject, the reader is referred to Arora (2004), Civicioglu (2013) and the references therein.

3.1 General concepts

The application of optimization in practical problems starts with the definition of, at least, one objective, which represents a performance measure of the system. In context of engineering structures, for instance, the target can be the reduction of its mass or volume, increase of its stiffness, among others. Then, the so-called design variables represent a certain group of the system characteristics that affect the pre-defined optimization goal. As a consequence, the main purpose of an optimization problem is to find the design variables that provide the best system performance, i.e., the minimum or maximum value of the objective function. In certain problems, the design variables can be constrained, originating a constrained optimization problem.

Hence, it is possible to characterize an optimization problem through the following elements:

a) Objective function: it is general a function, associated with the parameters of the analyzed problem, which measure the performance of the system. Taking as example a two bar truss submitted to load P, shown in Figure 12. The objective could be the minimization of its mass, written as $w = \rho_i \cdot l_i \cdot a_i$, where ρ_i is the specific mass, l_i is the length and a_i is the

cross sectional-area of each member i;

Figure 12 – Truss used as example

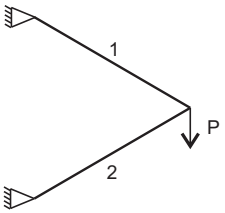

b) Design variables: they are the parameters allowed to be modified, in order to improve the objective function value. These variables can be written as the vector $\mathbf{x} = (x_1, ..., x_n)$. Where n is the number of variables and E is the associated design space. Using again the truss example of Figure 12, it is possible to define as design variables the value of cross sectional area of each member a_i. They can be grouped into a vector: $\mathbf{x} = (a_1, a_2)$.

c) design space: constraints are applied to the variables to limit the design space, determining a subspace S of E. Still using this truss example, it is possible to limit the values of cross sectional areas between minimum and maximum values, thus $a_{min} \leq a_i \leq a_{max}$. It is also possible to consider constraints regarding maximum or minimum nodal displacements.

The optimization problem can be written as:

$$\begin{aligned} Find \quad & \mathbf{x} \\ Which\ minimizes \quad & w(\mathbf{x}) \\ Subjected\ to \quad & \mathbf{x} \in S \end{aligned} \tag{3.1}$$

In the context of the optimization problem, some concepts are relevant, such as convexity and local minimum. In order to explain these concepts, let's consider the one variable function $f(x) = x^2$, shown in Figure 13. Note that if a straight line is constructed between any two points $(x_1, f(x_1))$ and $(x_2, f(x_2))$ on the curve, the line lies above the graph of $f(x)$ at all points between x_1 and x_2. This property characterizes convex functions Arora (2004). Through the geometry shown in Figure 13, the definition of convexity can be written as the inequation $f(x) \leq \alpha f(x_2) + (1-\alpha)f(x_1)$, where $x = \alpha x_2 + (1-\alpha)x_1$. This inequation can be written as:

Figure 13 – Convex funtion $f(x) = x^2$

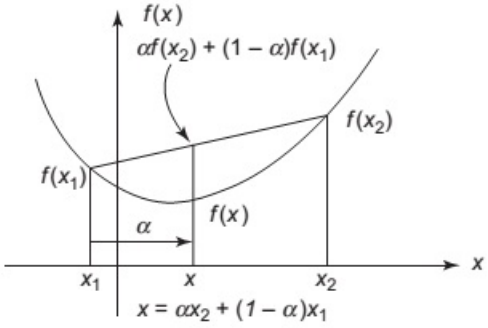

Source: Arora (2004, p. 151)

$$f(\alpha x_2 + (1-\alpha)x_1) \leq \alpha f(x_2) + (1-\alpha)f(x_1) \quad \text{for } 0 \leq \alpha \leq 1 \quad (3.2)$$

According to Arora (2004) this definition can be generalized to a function of n variables. A function $f(\mathbf{x})$ is convex if it satisfies the inequation:

$$f(\alpha \mathbf{x}^{(2)} + (1-\alpha)\mathbf{x}^{(1)} \leq \alpha f(\mathbf{x}^{(2)}) + (1-\alpha)f(\mathbf{x}^{(1)}) \quad \text{for } 0 \leq \alpha \leq 1 \quad (3.3)$$

These inequations represent a necessary and sufficient condition. In the context of engineering optimization, it is usually difficult to fulfill the convexity conditions. Then, non convex function results in occurrence of local and global minima. A point is defined as a local minimum of $f(x)$ when its value is the smallest one only in comparison with their surroundings. Figure 14 presents an example of non convex function with local and global minima. Therefore, the problem described in Equation 3.1 consists in finding the global minimum, i.e., find $\mathbf{x^*} \in S$ for which $F(\mathbf{x^*}) \leq F(\mathbf{x}) \; \forall \; \mathbf{x} \in S$.

Figure 14 – Global and local minima

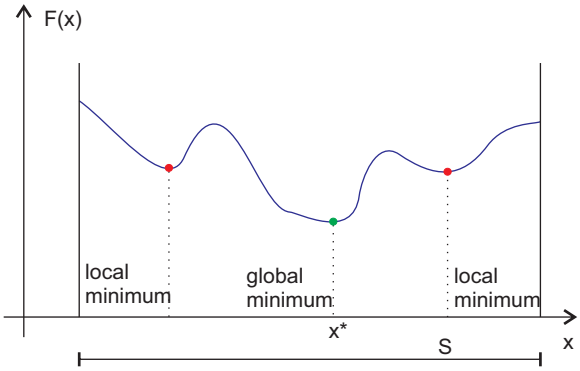

3.2 Optimization problems

The optimization problems can be classified into the following categories.

a) Regarding the convexity of the objective function

- Convex: when the objective function is convex. For these problems, the optimization problem can be solved through mathematical methods. Additionally, these methods have their convergence guaranteed and their global minimum

with mathematical prove (i.e. it is possible to prove if a given minimum is the global minimum);

- Non convex: when the objective function does not comply with the convexity condition. For these cases it is not possible to prove their global minimum and the convergence is not guaranteed. The great majority of engineering problems are non convex;

b) Regarding the design variables

- Continuous variables: which may assume any real value;
- Discrete variables: which may assume values that respect a given constraint;
- Mixed variables, involves both continuous and discrete variables.

3.3 Optimization algorithms

In general, optimization algorithms are based on iterative processes. They usually begin with an initial vector $\mathbf{x}_0$ of the variable $\mathbf{x}$ and follows the sequence $\mathbf{x}_0, \mathbf{x}_1, ..., \mathbf{x}_n$, until supposedly converge to the global minimum (or global maximum). The strategy employed to to determine each point of this sequence is what differentiates the optimization algorithms. The great majority of these strategies employ the objective function value, the constraints and the first and second order derivatives of these functions. Moreover, some algorithms also store information on the entire set during the iterations, while others only use information about the previous iteration. Thus, the optimization algorithms can be divided according to the information used to solve the problem.

a) Methods of order zero: use only the value of the objective function and constraints. For example:

- Dichotomy;
- Nelder-Mead;

- Standard genetic algorithms.

b) First order methods: also use the first derivative of the objective function and constraints. For example:

- Gradient method;
- Projected gradient method;
- Method of penalties;
- Augmented lagrangian method.

c) Second order methods: use the information of the second derivative of the objective function and constraints. For example:

- Newton's method.

The optimization algorithms can also divide as:

a) global: method which tries to converge to the global minimum;

b) local: method which converge to a local minimum.

There are several global and local optimization methods available in the literature. Among them, the most popular local methods are the descent methods, Newton's method and the direct method. Global methods usually involve the application of randomness, for instance, genetic algorithms, simulated annealing and random search (Lopez, Luersen & Cursi (2009a), Lopez, Luersen & Cursi (2009b)). There are also hybrid methods, which combine local and global strategies, such as those presented in Miguel, Lopez & Miguel (2013a), Finotto *et al.* (2013), Nhamage *et al.* (2014), Soleimani & Kannan (2015), and others.

To compare optimization algorithms, it is possible to address the following topics Nocedal & Wright (2006):

a) Efficiency: understood as the number of objective function evaluations, necessary to achieve convergence;

b) Robustness: capacity of the algorithm to find an optimum result, regardless the configuration of the problem and the starting point;

c) Accuracy: defined as the capacity of the algorithm to find an specific solution, without a significant sensibility related to its computational implementation.

These topics are often in conflict. For example, a method which is capable of a quick convergence, on an unconstrained and non-linear problem, may have a low accuracy. On the other hand, a more robust method may be too slow and inefficient. The relation between the efficiency, accuracy and robustness are the main questions in numerical optimization. It is important to highlight that one of the inherent characteristics of an optimization process is that there is not an universal method to solve all problems. Thus, it is the responsibility of the user to choose the suitable algorithm for each problem.

3.4 Heuristic algorithms

The presence of both continuous and discrete variables, as well as the non linear and non convex character of the shape optimization problem Torii, Lopez & Biondini (2012), lead to a problem with complex solutions, even considering simple trusses. The non linear and non convex characteristics, result on a problem where conventional optimization methods, gradient based for example, do not achieve satisfactory results. In this context, the so called Metaheuristic algorithms are well suited to deal with these types of problem. Besides the higher computational cost involved, these algorithms present the advantages of exempt the requirement of the function gradient and usually do not become trapped into local minimum, if correctly set Lopez, Luersen & Cursi (2009a),Miguel, Lopez & Miguel (2013b).

Due to these reasons, the *Backtrack search algorithm* (BSA), developed by Civicioglu (2013), is employed herein in order to perform the optimization. A brief explanation of the BSA is presented in the following sections. This choice was based on previous analysis and tests carried out with different metaheuristic algorithms. The BSA has shown a superior performance.

3.4.1 Backtrack search algortihm - BSA

The BSA is multi-agent based evolutionary algorithm developed by Civicioglu (2013), able to solve unconstrained non-convex optimization problems. It is thus employed in this study to address the optimization problems. A general overview of the BSA is illustrated in Table 1 and the details of each step are in the next subsections. The BSA description shown here is different from the original description given by Civicioglu (2013). The author hope that the description given here be more direct and easy to understand.

Table 1 – BSA pseudo-code

1. *Initialization*
Do
Generation of the perturbed/trial population
2. Evaluation of the direction/length of the perturbation
3. Perturbation of the current population
end
4. Selection of the new population
Until Convergence criteria are met

- Initialization

  The initial population P of BSA is generated as defined Equation 3.4:

$$(P)_{ij} \sim U(x_j^{min}, x_j^{max}) \tag{3.4}$$

  where U is a random variable uniformly distributed, x_j^{min} and x_j^{max} are the lower and upper bounds of the j^{th} design variable. $i = 1, \ldots, t_{pop}$ and $j = 1, \ldots, n_v$, where t_{pop} represents the size of the population and n_v the dimension of the problem. Thus, each row of P represents an individual of the population and each column represents a design variable. After the construction of the initial population the iterative process of the algorithm is initiated

by generating trial populations and updating them until some convergence criterion is achieved.

- Construction of the trial population P_{pert}

  The first step in the construction of the perturbed population (or trial population) P_{pert} is the evaluation of the *direction* of the perturbation that will be applied to the current population. Such a direction is calculated with the aid of the historical population P_{hist}. There are two possible cases for the evaluation of P_{hist}, each with a 50% of chance of happening. In case 1, P_{hist} is generated by a random permutation of the lines of the current population, while in case 2, it is randomly generated just as the initial population. This procedure is illustrated in Table 2, where a and b are random constants following a uniform distribution between zero and one, and := is an update operator. The author that proposed the BSA claimed that it has a memory from past iterations. Actually, this memory is due to the construction of P_{hist} using case 1. With P_{hist} at hand, the perturbed population P_{pert} is determined according to Equation 3.5:

Table 2 – Evaluation of P_{hist}

if $a < b \,\vert\, a, b \sim U(0,1)$	
then	
$\mathbf{P}_{hist} := \mathbf{P}$	|1st case: $\mathbf{P}_{hist}$ is the random
	| permutation of the lines
$\mathbf{P}_{hist} := randperm(P_{hist} :)$	| of the current $\mathbf{P}$
else	
$(P_{old})_{ij}\ U(lb_j, ub_j)$	| 2nd case: $\mathbf{P}_{hist}$ is randomly
	| restarted
end	

$$P_{pert} = P + M. * [\alpha(P_{hist} - P)] \tag{3.5}$$

in which the operator $.*$ holds for the multiplication term by term and α is a random parameter that controls the amplitude of the

search direction matrix $(P_{hist} - P)$. In the present study, α is generated through Equation 3.6:

$$\alpha = 3N \tag{3.6}$$

where N is a standard normal random variable (mean equal to zero and standard deviation equal to one). The purpose of the matrix M in Equation 3.5 is to define which terms of P are perturbed by $\alpha(P_{hist} - P)$ to generate the perturbed or trial population. That is, it is comprised by zeros and ones, and each term M_{ij} of M equal to one means that the corresponding term P_{ij} of P will be perturbed for the construction of the perturbed population P_{pert}

Initially, $\mathbf{M}$ is set as a $t_{pop} \times n_v$ zero matrix, and for the rest of its construction two cases may be applied at each iteration of the algorithm, each with a 50% chance of happening. In the first case, the parameter mix rate (m_r) chooses randomly up to m_r elements of each line of $\mathbf{M}$ to assume the unit value. In the second case, only one term of each line is randomly chosen to be equal to 1. The process just described for the construction of $\mathbf{M}$ is also illustrated in Table 3, in which $randi(n_v)$ is a discrete uniform random value between one and n_v.

As a result of the perturbation process some individuals of the perturbed population may extrapolate the boundaries of the design domain. Thus, at the end of this step, the individuals beyond the search-limits are randomly regenerated in the admissible design domain.

Table 3 – Generation of matrix M

$\mathbf{M} = zeros(t_{pop}, n_v)$	
if $a < b \,\vert\, a, b \sim U(0,1)$	|
then	|**Case 1**: $(m_r \; U \; n_v)$
for $i = 1 : t_{pop}$	| individual are perturbed
$\mathbf{M}_{i,u_{(1:\{m_r \, U \, nv\})}} = 1 \,\vert$	|
$u = randperm(\{1, 2, 3, \ldots, n_v\})$	
end	
else	|
for $i = 1 : t_{pop}$	|**Case 2**: only
$\mathbf{M}_{i,u_{randi(nv)}} = 1$	| 1 variable is perturbed
end	|
end	

- Selection of the new population

  In this step, the fitness value of each individual of the perturbed population P_{pert} is evaluated. Then, the algorithm compares the objective value of the the i^{th} individual $(P_{pert})_{(i,:)}$ of the perturbed population to the i^{th} individual $(P)_{(i,:)}$ of P. If the objective function of $(P_{pert})_{(i,:)}$ is better than the one of $(P)_{(i,:)}$, the latter is replaced by the former in the new population of the algorithm.

4 Topology optimization of transmission line towers

This chapter details the proposed templates based approach for topology optimization of TLTs. A general rule for the templates creation is also introduced, which is based in terms of the design practice and feasibility of prototype testing. Finally, the optimization formulation of the studied problem is illustrated.

4.1 Proposed approach for topology optimization

In the proposed approach, the structure is divided into main modules, which can assume different pre-established topologies (templates). Figure 15 illustrates how the pre-established templates are used for topology optimization. In this case, the structure was divided in three modules (parts): superior, intermediate and inferior. During the optimization process, the topology is optimized simultaneously to the size and shape, by choosing among the possible combination of templates, the ones that provide the lighter structures and fulfill the constraints. It is important to notice that through this idea it is also possible to use towers with staggered bracing.

Topologies with staggered bracing lead to an additional issue concerning the definition of the effective buckling lengths in the leg members of the structure. The buckling lengths are not simply given by the distance between two adjacent nodes when staggered bracing is used. This happens because the diagonals of a face do not prevent buckling in the plane corresponding to the other face. Observe in Figure 16 that $x-x$, $y-y$ and $z-z$ represent the local axes showed in the cross-sectional sketch. For the continuous bracing tower, the unbraced buckling length Lxx, Lyy or Lzz about $x-x$, $y-y$ and $z-z$ axes, respectively, is simply the distance between two adjacent nodes. Then,

Figure 15 – Topology optimization using templates (bracing bars are represented by dashed lines).

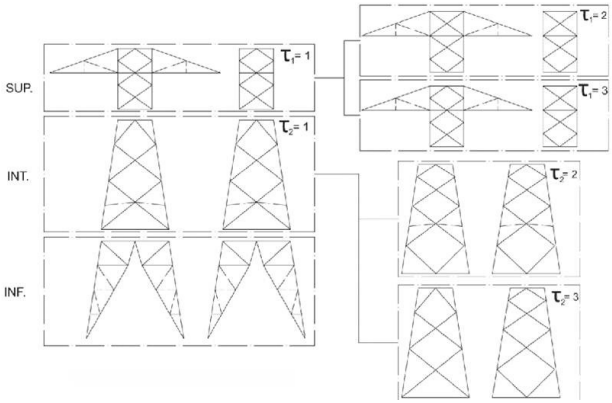

Figure 16 – Buckling length on structures with symmetry on four faces (left) and with staggered bracing (right).

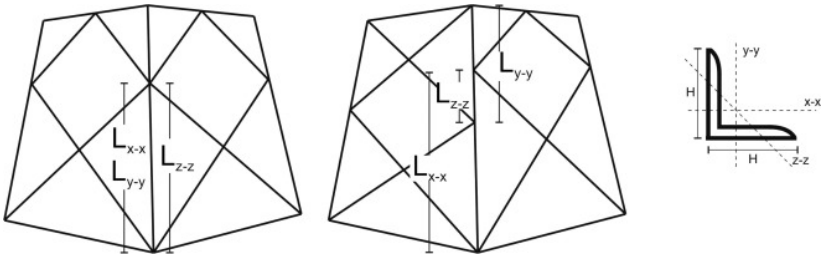

the buckling will occur about its minor principal axis $z - z$. On the other hand, considering the unbraced buckling lengths Lxx, Lyy or Lzz for the staggered bracing tower, illustrated in the Figure 16. It is not possible anymore to guarantee that the buckling will occur always about its minor principal axis $z - z$. Indeed, this definition will depend on the slenderness ratio Lxx/rxx, Lyy/ryy or Lzz/rzz, which must be assessed in each iteration of the optimization procedure.

Consequently, it is necessary to prescribe the correct effective buckling lengths together with the structural topology. In other approaches presented hitherto, the buckling lengths were evaluated directly from the structural model as the distance between two adjacent nodes. This seems to prevent the use of these approaches for the case of staggered bracing, where buckling lengths must be specified by the designer. In this work the buckling lengths can be defined together with each available template, allowing the correct modeling of local buckling during the optimization procedure even in complex cases as that of staggered bracing. Despite the presented idea does not seem to be complicated to implement, it is useful to generalize this concept. This can be carried out by providing a general rule for the templates creation procedure. Before presenting this scheme, it must be highlighted that these templates can be conceived considering previous design standard practices (e.g. staggered bracing) and limitations, while taking into account other practical aspects of importance (e.g. performance of the structure in prototype testing).

As experimentally demonstrated by CIGRÉ (2009) and discussed in Section 2.5, the topology plays an important role in the structural behavior observed in full-scale tests. Even small changes in the configuration (e.g. in the bracing pattern or in the position of the diaphragms) directly affect the structural behavior and the compatibility with the mechanical model adopted for the design. These and other aspects of main practical significance can be taken into account in the construction of the templates available for the optimization process. Through all these considerations, the template creation rules are shown in Figure 17 and described as follows:

Figure 17 – Template creation rule

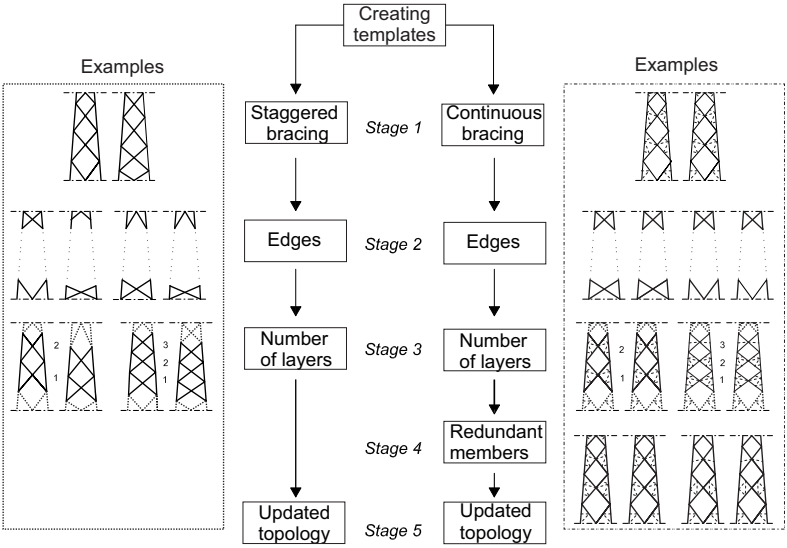

Stage 1. Choice of bracing patterns. (τ_1) The first design variable defines which bracing pattern will be chosen: continuous or staggered. These are the most common bracing patterns found in medium high transmission towers. The staggered bracing offers the advantage of eliminating the need for redundant members, however more diagonals are usually demanded.

Stage 2. Choice of the edges. (τ_2 and τ_3) The design variables τ_2 and τ_3 define the inferior and superior edges, respectively. As previously mentioned even small variations in the bracing edges can have a great influence on the structural behavior and consequently on the optimization result. Then, through this procedure the designer can determine all possible configurations or, for instance, limit to just a group of options that takes into account the performance of the structure in prototype testing.

Stage 3. Number of internal layers. (τ_4) The number of diagonal layers is also a design variable τ_4. In this aspect, there is the trade-off between the increase of structural capacity (resulted from the reduction of buckling length) and the increase of total weight.

Stage 4. Choice of redundant member. (τ_5) The configuration of redundant members is represented by the design variable τ_5. The redundant members are responsible for the reduction of buckling length. Note that they are only employed in towers with continuous bracing (depending on the definition of τ_1). This choice directly affects the final structure capacity due to the buckling length and its final weight.

The starting point and the bounds of the geometrical choices (τ_1, τ_2, τ_3, τ_4 and τ_5) provided to the optimization scheme, are defined based on the electrical clearance's requirements and design requirements (length a and length of the tower body $t.b.$ on Figure 18) and/or by the designer experience (the slope α, the angle θ, and the lengths of the inferior and superior edges $i.e.$ and $s.e.$). Moreover, these values typically depend on the type of the tower and its function in the transmission line.

Tangent towers in single or double circuit, with vertical or horizontal distribution of the conductors, used for voltages less than 500kV, represent the great majority of structures found in the Brazilian grid. In this case, the distance a typically assumes values between 1.0 and 1.5 meters, while its tower body ($t.b.$) varies from 6 to 18 meters. Then, structures may achieve around 50 m high, by connecting different extensions and leg sizes. For these structures, the design practice has shown that average values for α are around 4°, while values of $i.e.$ and $s.e.$ usually approach 2 and 0.5 meters, respectively. In addition, the angle θ presents a mean value of 90° for continuous bracing. Since it is adopted an almost constant angle for all diagonal layers, the leg buckling length is higher in the inferior part of the tower body than it is in the superior part. Then, to circumvent this difference, redundant members are employed.

Through these geometrical premises, the leg buckling length about

Figure 18 – Geometrical characteristics of the inclined tower body.

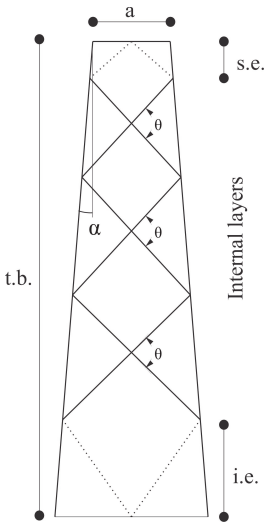

its minor axis is lead to around 1 meter in almost all tower body. On the other hand, in the staggered bracing pattern, a lower angle θ (or a greater number of layers) is required to maintain this buckling length configuration, since it avoids the use of redundant members.

It is important to highlight that even though these values are based on experience, they are valuable information for the template construction.

The strategy adopted in this study to calculate the interval of internal layers number, which will be provided for the optimization process, is shown on Figure 19. On this scheme, the values a, $t.b.$, α, θ, $i.e.$, and $s.e.$ should be fixed a priori. Then, the number of internal layers is promptly calculated simply following geometrical constraints. To allow expanding the search space for the optimization process, it is also furnished options with one more and one less layers than the previously determined. After defining the number of layers, the vertical coordinates of the internal nodes need to be provided. Then, it is

proposed the use of the regression curve (Figure 19) based on design experience, representing a proportion between the number of internal layers and the vertical coordinates.

For instance, defining a tower body with a, $t.b.$, α, $i.e.$, and $s.e.$ equal to 1 m, 12 m, 4°, 90°, 2 m and 0.5 m, respectively, the calculated number of internal layers would be 6 and the options provided to the optimization would be 5, 6 and 7. For each layer configuration, the vertical coordinates of the internal nodes are determined using the proposed regression equation. To apply this equation, firstly the edge distances ($i.e.$ and $s.e.$) are fixed in the horizontal axis. Then, the vertical nodes are uniformly distributed and the values obtained in the vertical axis will provide the initial nodal vertical coordinates of the tower body.

Due to the absence of redundant members (resulting in higher buckling lengths on the members), the staggered bracing demands an additional number of internal layers. Thus, the internal layer interval is defined based on the continuous bracing, simply by increasing one unity to each option. Consequently, the options for this example with staggered bracing would be: 6, 7 and 8 internal layers. Figure 20 presents an example with the same parameters used for the continuous bracing, yet considering 7 internal layers (one more comparing to the continuous bracing). As shown in Figure 20, first, the internal nodes of the longitudinal face are defined though the same strategy applied for the continuous bracing, while employing a different regression equation. Thereafter, the internal nodes of the transverse face are taken in the midpoints of the longitudinal face.

Finally, another important advantage of this scheme is that the search space is limited and only the most common topologies employed by the industry can be provided as templates. Indeed, the idea of reducing the search space was already employed by other researches as previously mentioned. For example, Shea & Smith (2006) and Guo & Li (2011) have employed this idea in previous attempts of proposing methods for topology optimization of transmission line towers. Thus, the

Figure 19 – Number of internal layers and internal nodes configuration for continuous bracing.

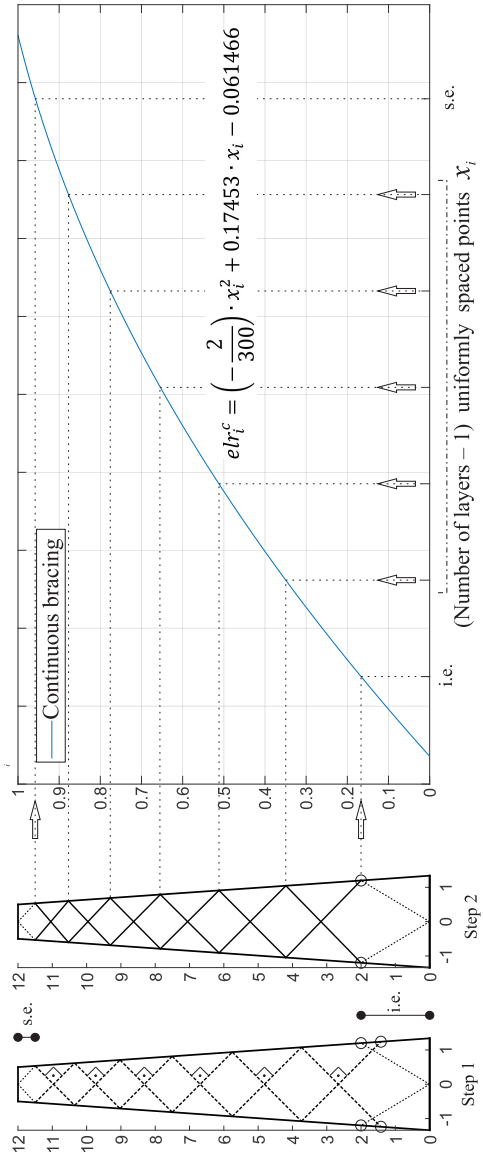

Figure 20 – Number of internal layers and internal nodes configuration for continuous bracing.

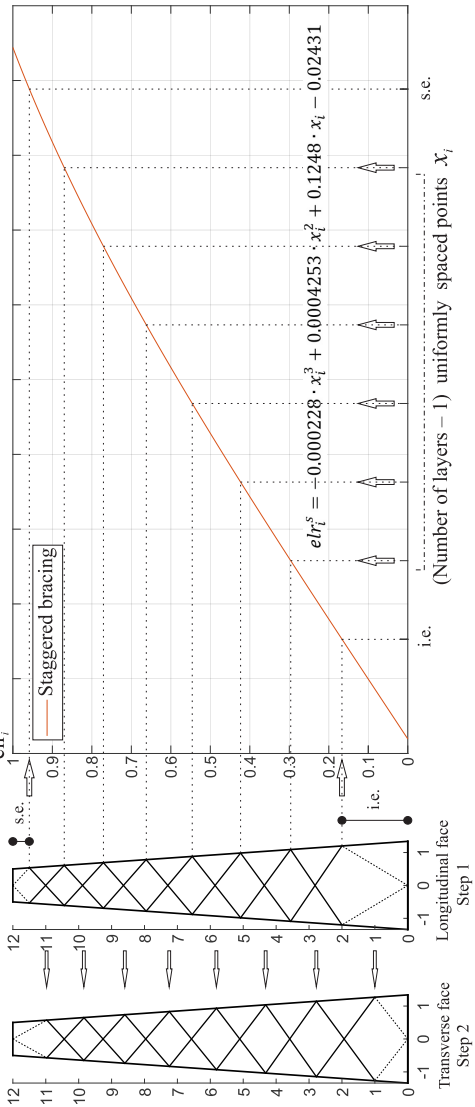

present study goal is to keep the advantages of limiting the search space (to fulfill constructional requirements and reduce the computational cost), while introducing the templates based optimization concept, which allows advantages such as the proper consideration of important practical details in the topology as observed by CIGRÉ (2009) and a staggered bracing configuration.

4.2 Optimization formulation

During the process, the optimization variables are stored in the vector $\mathbf{x}$. For size optimization the cross sectional areas of the structural members are taken as the design variables, represented as the vector $\mathbf{a}$. The coordinates of some chosen nodes are taken as design variables for shape optimization, and stored in vector $\boldsymbol{\xi}$. For practical purposes, the design variables related to nodal coordinates are taken as discrete values. Finally, the topology vector $\boldsymbol{\tau}$ is used to store the templates employed in each module of the structure. The final vector of design variables is $\mathbf{x} = \{\mathbf{a}, \boldsymbol{\xi}, \boldsymbol{\tau}\} = \{a_1, \ldots, a_m, \xi_1, \ldots, \xi_q, \tau_1, \ldots, \tau_s\}$, where m is the number of cross-sectional areas, q is the number of nodal coordinates and s is the number topology variations taken as design variables. The aim of the optimization problem is to minimize the structural weight while respecting the imposed constraints. Therefore, the problem previous mentioned (Equation 3.1 in Chapter 3), can now be written as Equation 4.1:

$$\begin{aligned}
&\textbf{Find} \quad \mathbf{x} = \{a_1, \ldots, a_m, \xi_1, \ldots, \xi_q, \tau_1, \ldots, \tau_s\} \\
&\textbf{That minimizes} \quad w = \sum_{i=1}^{m} \rho_i l_i(\mathbf{x}) a_i(\mathbf{x}) \\
&\textbf{Subjected to load constraints} \\
&g_i(\mathbf{x}) = |S_{di}(\mathbf{x})| - R_{di} \leq 0, \ (i = 1, 2, \ldots, m), \\
&\textbf{Slenderness constraints} \\
&g_{i+m} = \lambda_t(\mathbf{x}) - \bar{\lambda_t} \leq 0, \ (i = 1, 2, \ldots, m) \\
&\textbf{and cross sectional constraints} \\
&g_{i+2m}(\mathbf{x}) = \frac{w_i(\mathbf{x})}{t_i(\mathbf{x})} - w/t_{max}
\end{aligned} \tag{4.1}$$

where W is the structural weight, and for a given bar i, ρ_i is the specific weight of the material, l_i is the length of each bar, S_{di} is the factored load in each bar, R_{di} is the factored resistance of each bar, λ_i is the slenderness ratio of each bar, $\bar{\lambda_i}$ is the allowable slenderness ratio of each bar, t_i is the thickness of each bar, w_{fi} is the flat width of each angle profile leg and w_f/t_{max} is the allowable relation between w and t for each bar.

The Appendix, in section 7, describes the determination of the values for the load, slenderness ratio and cross sectional area constraints.

A penalization scheme is used to transform the constrained optimization problem given by Equation 4.1 into an unconstrained problem. Hence, the objective function (weight) of unfeasible solutions are penalized by a parameter P_t . It is important to carefully choose the penalization in order to avoid convergence issues of the search algorithm. Taking P_t too high can prevent the convergence of the algorithm, while taking it too small may not be enough to avoid unfeasible solutions. For this reason, the penalization is defined as a function of overall constraint

violation, according Equation 4.2:

$$P_t(\mathbf{x}) = h\left[\sum_{i=1}^{m}\left(\frac{|S_{di}(\mathbf{x}) - R_{di}|}{\bar{\sigma}_i}\right)^{+} + \right] \left[+\sum_{i=1}^{m}\left(\frac{|\lambda_i(\mathbf{x}) - \bar{\lambda}_i|}{\bar{\lambda}_i}\right)^{+} + \sum_{i=1}^{m}\left(\frac{\frac{w_{fi}(\mathbf{x})}{t_i(\mathbf{x})} - \frac{w_f}{t_{max}}}{\frac{w_f}{t_{max}}}\right)^{+}\right] \tag{4.2}$$

where h is a positive constant parameter, with value 10^8, characterizing a technique of constraint handling called death penalty (i.e. the designs outside the admissible domain are excluded from search) Mezura-Montes & Coello (2011). Additionally, $(.)^+$ represents the operation in Equation 4.3.

$$(.)^+ = \frac{|(.)| + (.)}{2} \tag{4.3}$$

As previously mentioned, due to the discrete variables and the non-convex and nonlinear characteristic of this problem, a metaheuristic algorithm BSA was employed in order to perform the optimization.

5 Numerical examples

To illustrate the proposed topology optimization procedure, as well as show the templates creation scheme, two numerical examples are assessed.

5.1 115kV transmission line tower

A transmission line tower regularly found in Brazil is used as example in order to apply the proposed templates creation scheme. The structure is a single circuit, self-supported 115kV. The tower geometry and the locations of the redundant members are shown in Figure 22. The minimum phase to steel clearance requirements and the height of the tower peak above the cross arms (based on shielding considerations for lightning protection) are shown in Figure 21, this information is necessary to define the limits for the variations of shape. The available angle profiles employed in the optimization procedure are given in Table 4 and the steel adopted in the design was the ASTM A572 g 50.

The structure was subjected to two load cases, as shown in Figure 23. The first (a) is a transversal wind load hypothesis, which consists of the wind loads transmitted by the conductors and insulators as well as the wind loads acting on the support itself. For the wind load applied on tower, a uniform wind pressure of 1716 N/m^2 and a drag coefficient equals to 2 were adopted, in accordance with the original design. The second (b) represents a cable conductor rupture scenario, being composed of a 21994 N load applied on the top cross arm in the longitudinal direction. Finally, an overload shown in Figure 23 is considered for both cases.

An iterative process is proposed in the present study to calculate the wind loads on supports. This is due to the fact that the projected area of members is modified during the optimization process. Thus,

Figure 21 – Minimum phase to steel clearance.

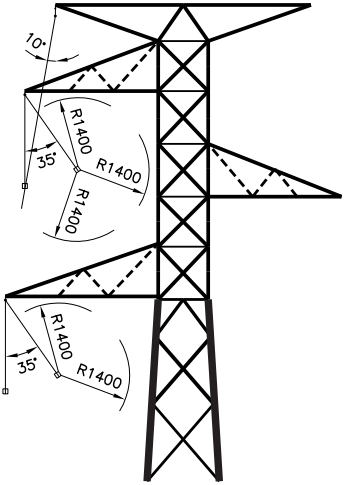

Table 4 – Available profiles for the optimization procedure

Profile (mm)	Area (cm^2)
L 40 × 40 × 3.0	2.35
L 45 × 45 × 3.0	2.66
L 50 × 50 × 3.0	2.96
L 40 × 40 × 4.0	3.08
L 45 × 45 × 4.0	3.49
L 40 × 40 × 5.0	3.79
L 50 × 50 × 4.0	3.89
L 60 × 60 × 4.0	4.71
L 65 × 65 × 4.0	5.13
L 60 × 60 × 5.0	5.82
L 65 × 65 × 5.0	6.31
L 75 × 75 × 5.0	7.36
L 75 × 75 × 6.0	8.75
L 75 × 75 × 7.0	10.1
L 90 × 90 × 6.0	10.6

Figure 22 – 115kV transmission line tower design.

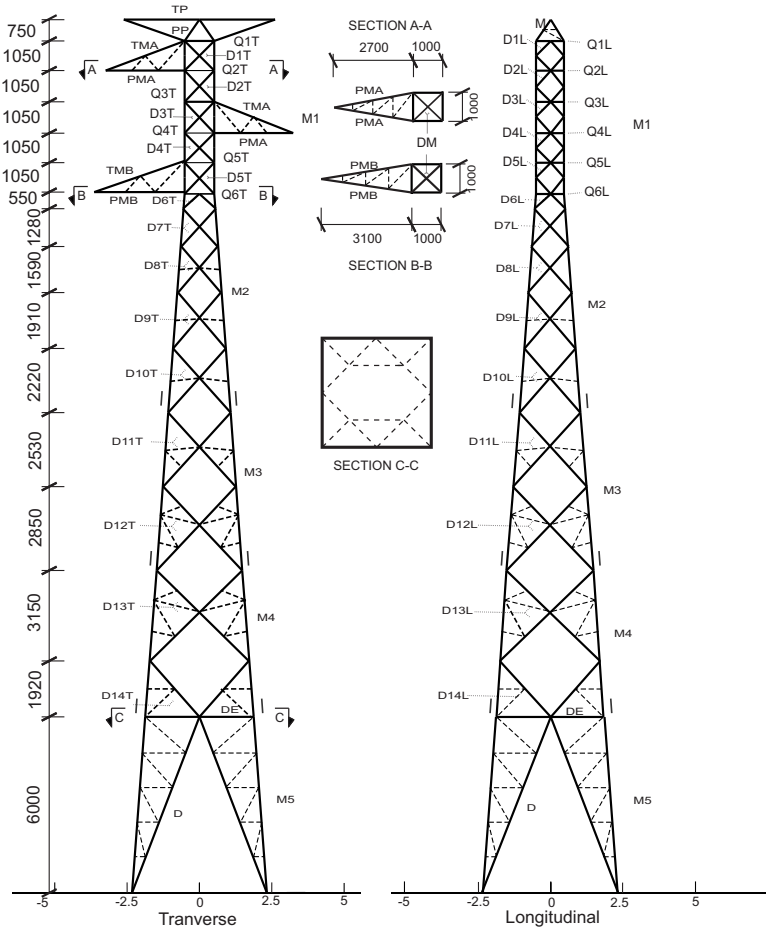

the wind load is updated in each optimization iteration. Through this procedure, the optimal structure will be subjected to a wind load evaluated according to its true projected area. In previous work reported in the literature (Shea & Smith (2006), Parıs *et al.* (2010), Guo & Li (2011), Parıs *et al.* (2012)) the wind load applied on the optimization

Figure 23 – Load cases.

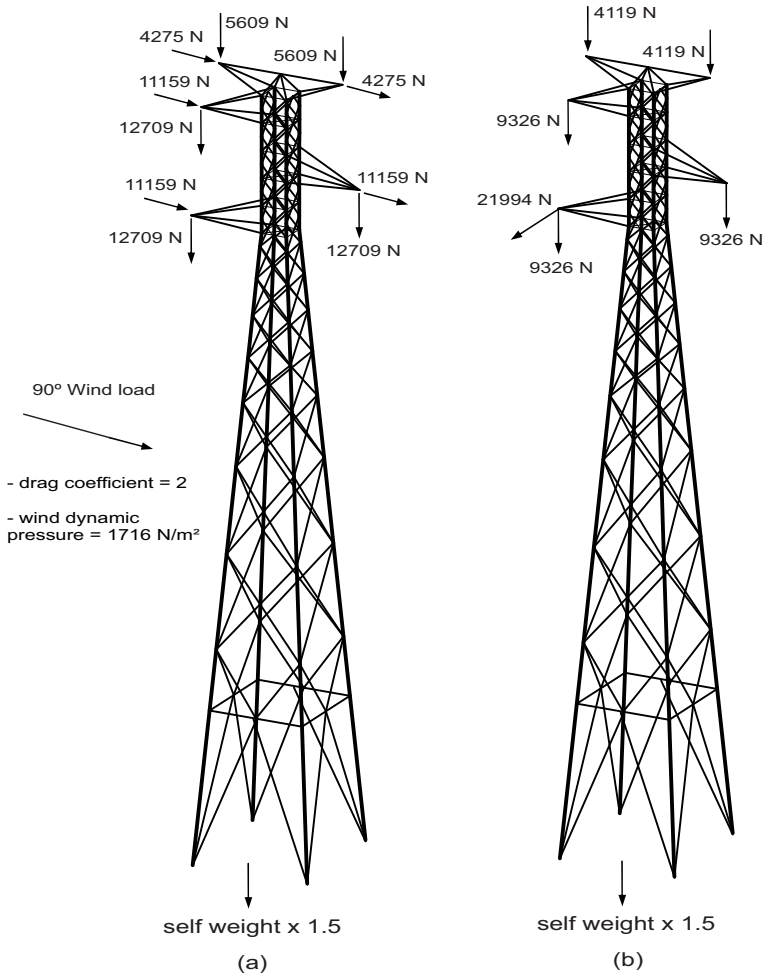

was a fixed value determined for the original design. Note that through this consideration an original design is always required. However, for a new structure, in which the wind load is totally undetermined, the iterative approach adopted in the present work is the only way to

correctly optimize the tower.

Note that in this example a uniform wind load and a constant drag coefficient were adopted in order to follow the original design. Nevertheless, the iterative scheme also works with wind load based on codes (for instance, IEC (2003) that employs the so-called solidity ratio to determine drag coefficients).

The structural analysis was performed through an in-house FEM routine developed in MATLAB. The towers were modeled using a combination of three dimensional truss and frame elements, considering elastic-linear analysis, small displacements and small deformations. Figure 24 presents the final model, in which the truss elements are represented in blue while the frame elements (main legs and diaphragms) are represented in red. Because the topologies employed in the present work are based on the current industrial practice, it is expected that bending stresses will not be significant Kaminski-Jr (2007). Then, their contributions were not added to determine the stresses in the elements. On the other hand, using this model the presence of planar joints was avoided.

Figure 24 – Final model for the 115kV tower.

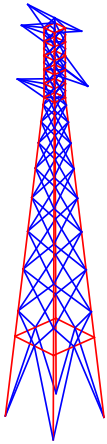

To clearly understand the influence of the optimization procedure in the final result, three separated studies were performed: i) size optimization; ii) size and shape optimization; iii) size, shape and topology optimization. Then, to assess the correct influence of each optimization level in the tower weigh reduction, the results provided in (ii) and (iii) will be compared to that obtained in (i) and not to the original structure weigh.

In all scenarios the BSA was employed. The BSA parameters were set as: $m_r = 1$, Population size $t_{top} = 30$ and number of cycles $C = 6000$, resulting in 180,000 OFE.

5.1.1 Size optimization

The bars were grouped as shown in Figure 22 for constructional reasons, totalizing fifty-four design variables. The vector of design variables is then defined as $\mathbf{x} = \{a_1, \ldots, a_{54}\}$, where a_i is the cross-sectional area of each group. Fifteen angle profiles with cross-sectional areas presented in Table 4 are available for each design variable.

Figure 25 – Typical convergence history for size optimization.

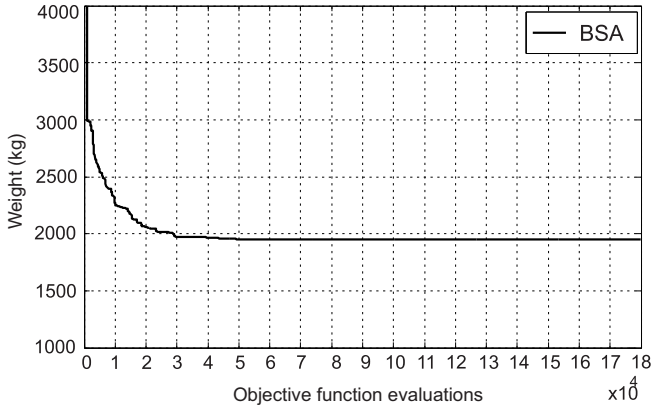

Table 5 – ts for size optimization

GROUP	Area(cm^2)	GROUP	Area(cm^2)
PP	2.35	D4T	2.35
PMa	2.35	D5T	2.35
TMa	2.35	D6T	2.35
PMb	3.89	D7T	2.35
TMb	2.66	D8T	2.66
M	2.35	D9T	2.66
M1	2.66	D10T	2.96
M2	6.31	D11T	2.66
M3	7.36	D12T	2.35
M4	7.36	D13T	2.35
D1L	2.35	D14T	2.66
D2L	2.35	Q1T	2.35
D3L	2.35	Q2T	2.35
D4L	2.35	Q3T	2.35
D5L	2.35	Q4T	2.35
D6L	2.66	Q5T	2.35
D7L	2.66	Q6T	2.66
D8L	2.66	Q1L	2.35
D9L	2.96	Q2L	2.35
D10L	2.96	Q3L	2.35
D11L	2.96	Q4L	2.35
D12L	2.66	Q5L	2.35
D13L	2.66	Q6L	2.35
D14L	2.66	DM2	2.35
D1T	2.35	DE	2.96
D2T	2.35	D	2.66
D3T	2.35	M5	8.75
Total weight (kg)	1950.5		
Average* (kg)	1950.8		
S.D.* (kg)	0.1393		
Reduction (%)	-		

*Statistical results for 25 runs.

The results of size optimization obtained by BSA are presented in Table 5, as well as the average value and the standard deviation calculated from 25 independent runs of the algorithm. The best result was 1950.5 kg while the average value was 1950.8 kg and 0.1393 kg

was the standard deviation. A typical convergence history for size optimization is shown in Figure 25.

A detailed analysis of the ratio between the elements internal forces and their capacities confirmed that the optimization led the cross-sectional areas of the bars to their lowest admissible angle profiles. Then, this optimal result will be taken as the reference value to assess the weight reduction obtained with size and shape and size, shape and topology procedures.

5.1.2 Size and shape optimization

It is recognized that the slope of the tower leg from the waist down has a significant influence on the tower. Thus, it is expected better results than that achieved only by size optimization. In addition, the vertical nodal coordinates of the inclined tower body were also considered as design variables.

The shape variation scheme is presented in Figure 26. The variation 1 (stored in the design vector as ξ_1) allows the base nodes to move horizontally. Variation 2 (stored in the design vector as ξ_2 to ξ_9) allows the nodes of the inclined tower body to move vertically, considering an independent variable for each layer (represented on Figure 26 by Var. 2.1, 2.2, 2.3, 2.4, 2.5, 2.6, 2.7, 2.8). Variation 3 (stored in the design vector as ξ_{10}) allows the superior part to move uniformly on the horizontal axis. The design vector is now $\mathbf{x} = \{a_1, \ldots, a_{54}, \xi_1, \xi_2, \xi_3, \xi_4, \xi_5, \xi_6, \xi_7, \xi_8, \xi_9, \xi_{10}\}$, where ξ_i represents the distance the nodes are shifted from their original position by the optimization algorithm. The lower and upper bounds imposed on the variations ξ_1, ξ_2 to ξ_9 and ξ_{10} are, respectively, $[-30, 30](cm)$, $[-30, 30](cm)$ and $[-10, 10](cm)$. Aiming a final result closer to a industrial application, ξ_i is allowed to assume discrete values at each 1 centimeter. Furthermore, the bounds for shape modifications Var. 1 and Var. 3 were determined based on the minimum phase to steel clearance requirements and the height of the tower peak above the cross arms. The bounds for Var. 2 were defined in order to allow a significant shape variation, while preventing the layers to overlap.

Figure 26 – Shape variation scheme.

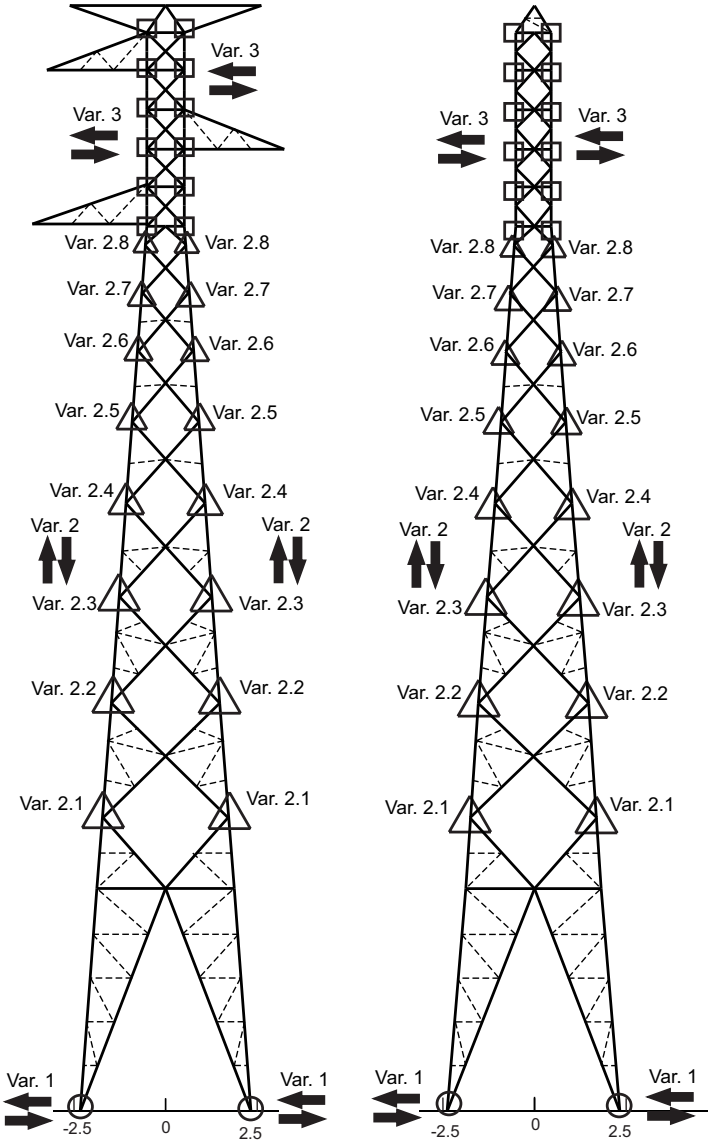

The cross-sectional areas and the geometrical variations for the optimal results found with BSA are presented in Table 6, as well as the average value and the standard deviation calculated from 25 independent runs. The best result was 1880.4 kg while the average value was 1891.0 kg and 6.22 kg as the standard deviation. As expected, the structural weight was reduced in comparison with the one obtained with size optimization only. Figure 27 presents a typical convergence history for size and shape optimization.

Table 6 – Optimal results for size and shape optimization

GROUP	Area(cm^2)	GROUP	Area(cm^2)	SHAPE VAR.	Var. (m)
PP	2.35	D4T	2.35	Var. 1	-0.22
PMa	2.35	D5T	2.35	Var. 2.1	0.12
TMa	2.35	D6T	2.35	Var. 2.2	0.04
PMb	3.89	D7T	2.35	Var. 2.3	0.17
TMb	2.66	D8T	2.66	Var. 2.4	0.19
M	2.35	D9T	2.66	Var. 2.5	-0.09
M1	2.66	D10T	2.66	Var. 2.6	-0.06
M2	5.82	D11T	2.66	Var. 2.7	0.03
M3	7.36	D12T	2.66	Var. 2.8	0.04
M4	7.36	D13T	2.35	Var. 3	-0.03
D1L	2.35	D14T	2.66		
D2L	2.35	Q1T	2.35		
D3L	2.35	Q2T	2.35		
D4L	2.35	Q3T	2.35		
D5L	2.35	Q4T	2.35		
D6L	2.35	Q5T	2.35		
D7L	2.66	Q6T	2.66		
D8L	2.96	Q1L	2.35		
D9L	2.96	Q2L	2.35		
D10L	2.96	Q3L	2.35		
D11L	2.96	Q4L	2.35		
D12L	2.66	Q5L	2.35		
D13L	2.35	Q6L	2.35		
D14L	2.66	DM2	2.35		
D1T	2.35	DE	2.66		
D2T	2.35	D	2.66		
D3T	2.35	M5	8.75		
Total weight (kg)	1880.4				
Average* (kg)	1891.0				
S.D.* (kg)	6.22				
Reduction (%)	3.59				

*Statistical results for 25 runs.

Figure 27 – Typical convergence history for size and shape optimization.

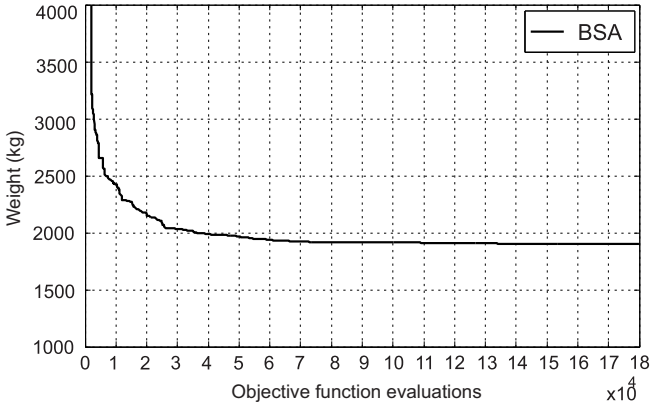

5.1.3 Size, shape and topology optimization

For this case, the templates creation procedure was employed. The topological variation is carried out in the inclined tower body. To apply the general creation rule the four stages previously explained must be defined. In **stage 1** both continuous and staggered bracing pattern were chosen. Then, the design variable τ_1 can assume values $\{0, 1\}$, being 0 for continuous or 1 for staggered bracing. In **stage 2**, 4 possibilities of inferior and superior edges were provided to the staggered bracing tower, resulting in a total of 16 combinations. In this case, the design variables τ_2 and τ_3 can assume values $\{1, 2, 3, 4\}$. Due to its symmetry, the continuous bracing tower has 3 possibilities of inferior and 2 for superior edges, resulting in 6 possible configurations. Then, the design variable τ_2 can assume values $\{1, 2, 3\}$ while τ_3 $\{1, 2\}$. The options are presented in Figure 28. Note that the designer can choose the number and the geometry of the edges. This has the advantage to take into account the constructional issues presented by CIGRÉ (2009).

Figure 28 – Edges for continuous and staggered bracing.

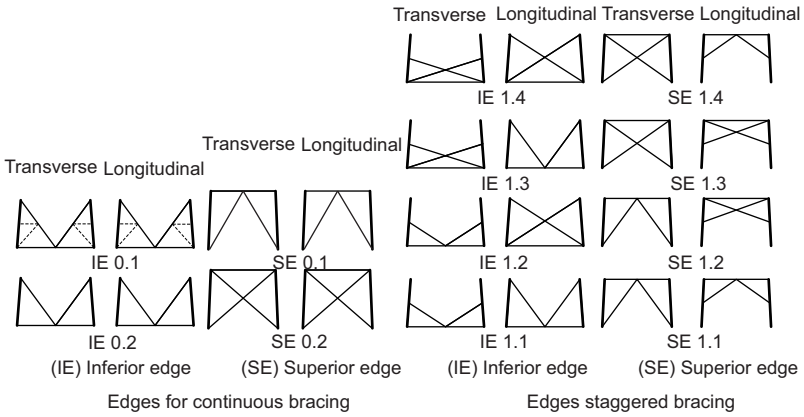

The number of internal layers (**stage 3**) were calculated based on the strategy mentioned on Chapter 4, by taking the geometrical values a, $t.b.$, α, $i.e.$ and $s.e.$ equal to the original design (1.0 m, 18 m, 4.332°, 1.92m and 0.55m, respectively). Through these parameters and adopting $\theta = 90°$, the number of calculated layers was 8. Then, the options with 7 and 9 were also provided, i.e., the design variable τ_4 can assume values $\{7, 8, 9\}$. The regression curve illustrated in Figure 19 was employed to define the starting point of the tower body vertical nodal coordinates. Note that the locations of the nodes corresponding to the edges are fixed, i.e., the values of $i.e.$ and $s.e.$ are taken as the original design (1.92m and 0.55m). Thus, for 7 internal layers, there are 2 fixed nodes (corresponding to the edges) and 6 internal nodes with initial vertical coordinates determined by the regression curve.

For the staggered bracing, an interval with one more layer than for continuous bracing was provided, consequently, the design variable τ_4 can assume values $\{8, 9, 10\}$. This choice was justified to keep buckling lengths of the tower legs in the same order of magnitude. The values $i.e.$ and $s.e.$ were also fixed as 1.92 and 0.55 meters, respectively. To

Figure 29 – Variation of internal layers number.

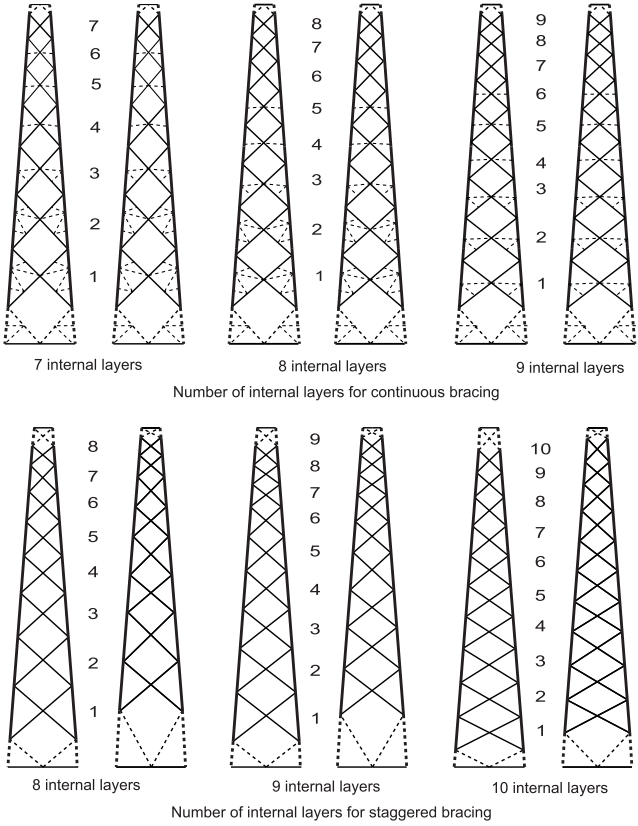

determine the vertical coordinates of the internal nodes, the appropriate regression equation for this case was used, which is presented on Figure 20.

The configurations of the different options of internal layers are presented in Figure 29. Note that the edges presented on the mentioned Figure were randomly chosen, only to illustrate the number of internal layers.

In **stage 4**, the configuration of the redundant members was kept unchanged. Thus, each one of the 3 internal layers possibilities given for the continuous bracing tower has a fixed redundant member configuration, which are presented in Figure 29. Finally, there are a total of 66 possibilities of topologies provided to the algorithm. An overview of the procedure is shown in the flowchart of Figure 30.

The optimal results obtained are presented in Table 7, while the convergence history for a typical run for size, shape and topology optimization is shown in Figure 32. The best result found was 1809.8 kg, the average result for 25 runs was 1887.9 kg and the standard deviation was 27.43 kg. This higher value of standard deviation (compared with the results for size and shape optimization, in Section 5.1.2) can be attributed to the significant increase of possible solutions, provided by the topology variation. Additionally, one can notice that the average value found in this case is similar (but yet lower) to the result for size and shape optimization.

It is important to highlight that the best topology obtained corresponds again to a structure with staggered bracing. In addition, it was possible to find 7.22% of weight reduction, when compared to only size optimization. Note that this value represents a real gain, because the geometrical and topological configuration of the original tower already presents the minimum weight possible. The design related to the best result is presented on Figure 31.

A final test was conducted to assess the optimum size, shape and topology design considering only structures with continuous bracing. Figure 33 presents the best result found, which was 1874.1kg and corresponds to a structure with one more internal layer than the original topology. This illustrates the capability of optimization scheme to create and offer economical topology solutions, because it found two better topologies than the original design. In addition, they are both in accordance with constructional requirements and prototype testing.

Figure 30 – Creation of templates.

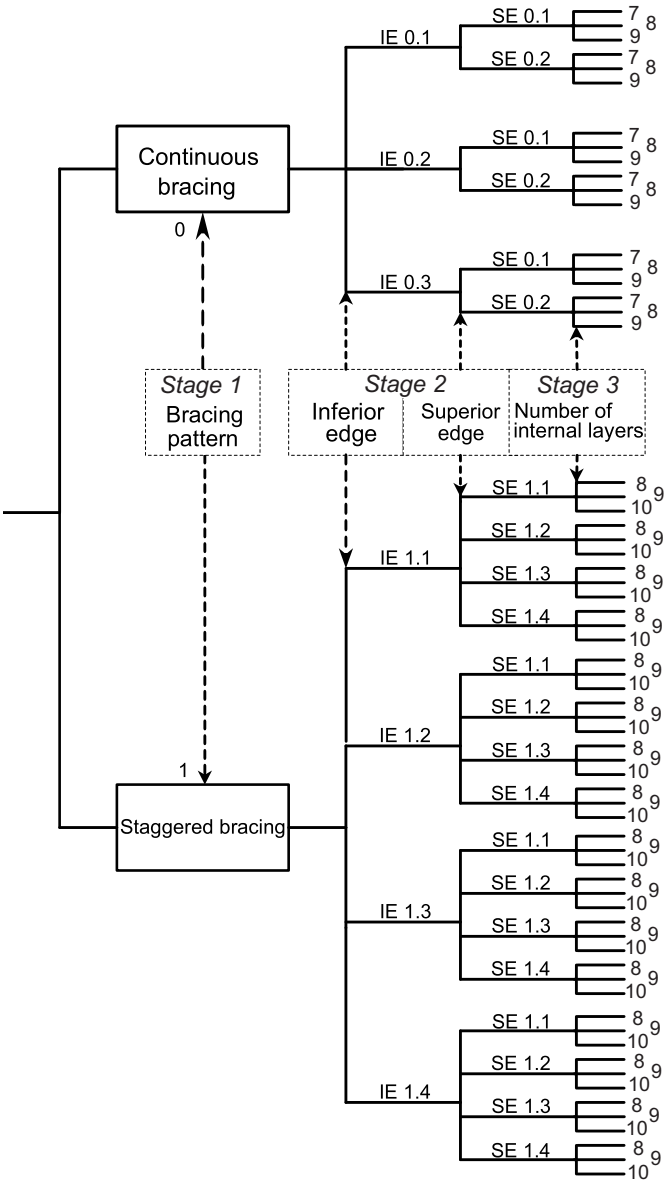

Figure 31 – Design of the best result for size, shape and topology optimization.

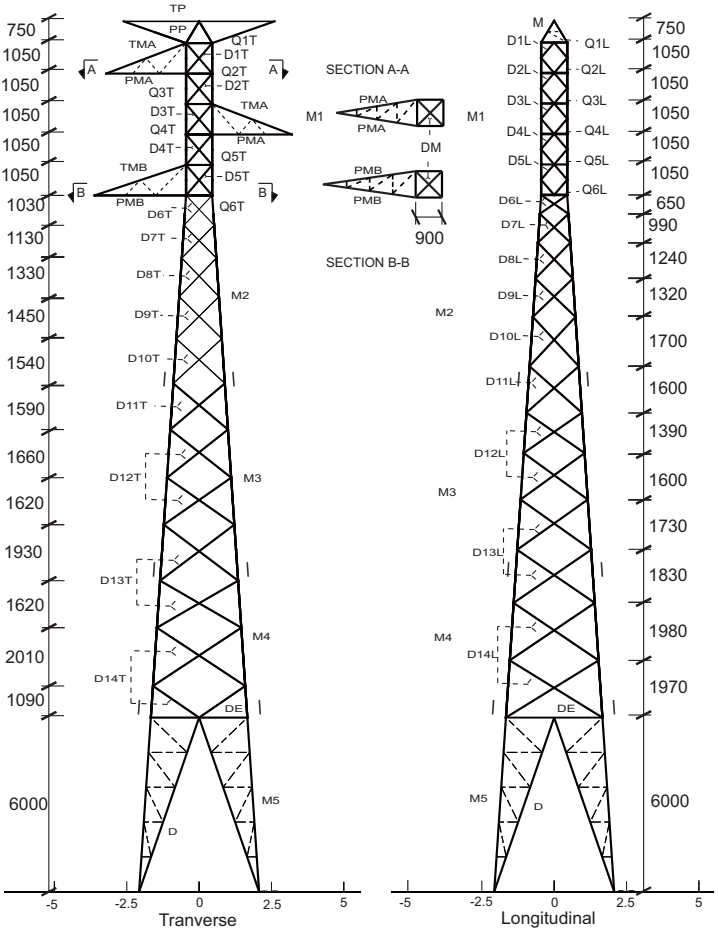

Furthermore, a regular design carried out by a senior engineer takes at least one week, while the presented optimization scheme requires around 5h of computational time, for each independent run, in a hardware configuration Intel Core i7 3.5GHz with 8 GB of RAM.

Figure 32 – Typical convergence history for size, shape and topology optimization.

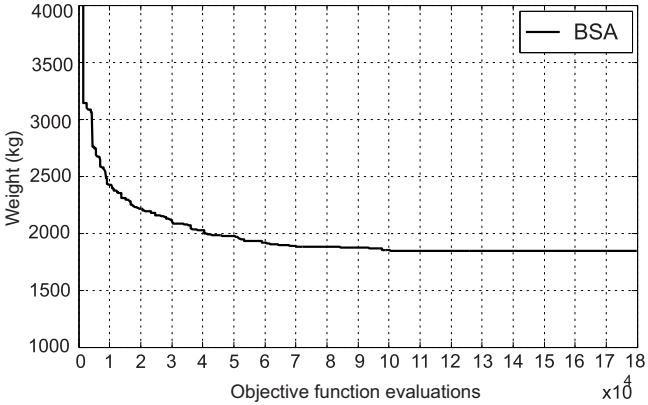

Table 8 shows the best results obtained for the three cases studied and the weight reduction percentage in comparison to only size optimization. It must be highlighted that topology optimization indeed allows a significant improvement of the structural design.

Table 8 – Best results for the three cases studied

Optimization	Weight (kg)	% reduction
Size	1950.5	-
Size and shape	1880.4	3.59%
Size, shape and topology	1809.8	7.22%

5.2 230kV transmission line tower

As a second example, another transmission line tower regularly found in Brazil is considered. The structure is a single circuit, self-supported 230kV. The geometry and the locations of the redundant members are shown in Figure 34. The minimum phase to steel clearance requirements and the height of the tower peak above the cross arms

Figure 33 – Design of the best result with continuous bracing for size, shape and topology optimization.

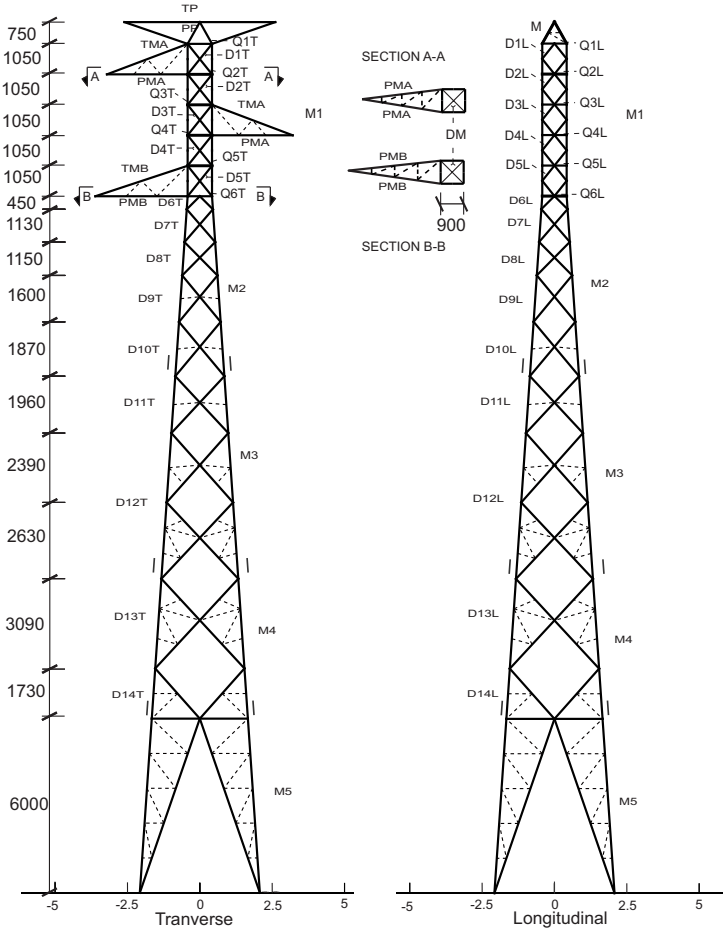

Table 7 – Optimal result for size, shape and topology optimization

GROUP	Area(cm^2)	GROUP	Area(cm^2)	SHAPE VAR.	Var. (m)
PP	2.35	D4T	2.35	Var. 1	-0.25
PMa	2.35	D5T	2.35	Var. 2.1	0.13
TMa	2.35	D6T	2.35	Var. 2.2	0.05
PMb	3.89	D7T	2.35	Var. 2.3	0.28
TMb	2.66	D8T	2.35	Var. 2.4	0.24
M	2.35	D9T	2.35	Var. 2.5	0.12
M1	2.96	D10T	2.35	Var. 2.6	0.3
M2	6.31	D11T	2.35	Var. 2.7	0.3
M3	8.75	D12T	2.35	Var. 2.8	0.29
M4	8.75	D13T	2.66	Var. 2.9	0.2
D1L	2.35	D14T	2.96	Var. 2.10	0.2
D2L	2.35	Q1T	2.35	Var. 2.11	0.2
D3L	2.35	Q2T	2.35	Var. 2.12	-0.05
D4L	2.35	Q3T	2.35	Var. 2.13	0.18
D5L	2.35	Q4T	2.35	Var. 2.14	-0.02
D6L	2.35	Q5T	2.35	Var. 2.15	0.2
D7L	2.35	Q6T	2.35	Var. 2.16	0.19
D8L	2.35	Q1L	2.35	Var. 2.17	0.2
D9L	2.35	Q2L	2.35	Var. 2.18	0.12
D10L	2.66	Q3L	2.35	Var. 2.19	0.2
D11L	2.66	Q4L	2.35	Var. 2.20	0.08
D12L	2.66	Q5L	2.35	Var. 2.21	0.1
D13L	2.66	Q6L	2.35	Var. 2.22	-0.1
D14L	2.96	DM2	2.35	Var. 3	-0.05
D1T	2.35	DE	2.66	TOPOLOGY VAR.	
D2T	2.35	D	2.66	τ_1	1
D3T	2.35	M5	8.75	τ_2	2
Total					
weight (kg)	1809.8			τ_3	3
Average* (kg)	1887.9			τ_4	10
S.D.* (kg)	27.43				
Reduction (%)	7.22%				

*Statistical results for 25 runs.

(based on shielding considerations for lighting protection) are shown in Figure 35, this information is necessary to define the limits for the variations of shape. The available angle profiles employed in the optimization procedure are given in Table 9 and the steel adopted in the design was te ASTM A572 g 50.

Figure 34 – 230kV original tower design.

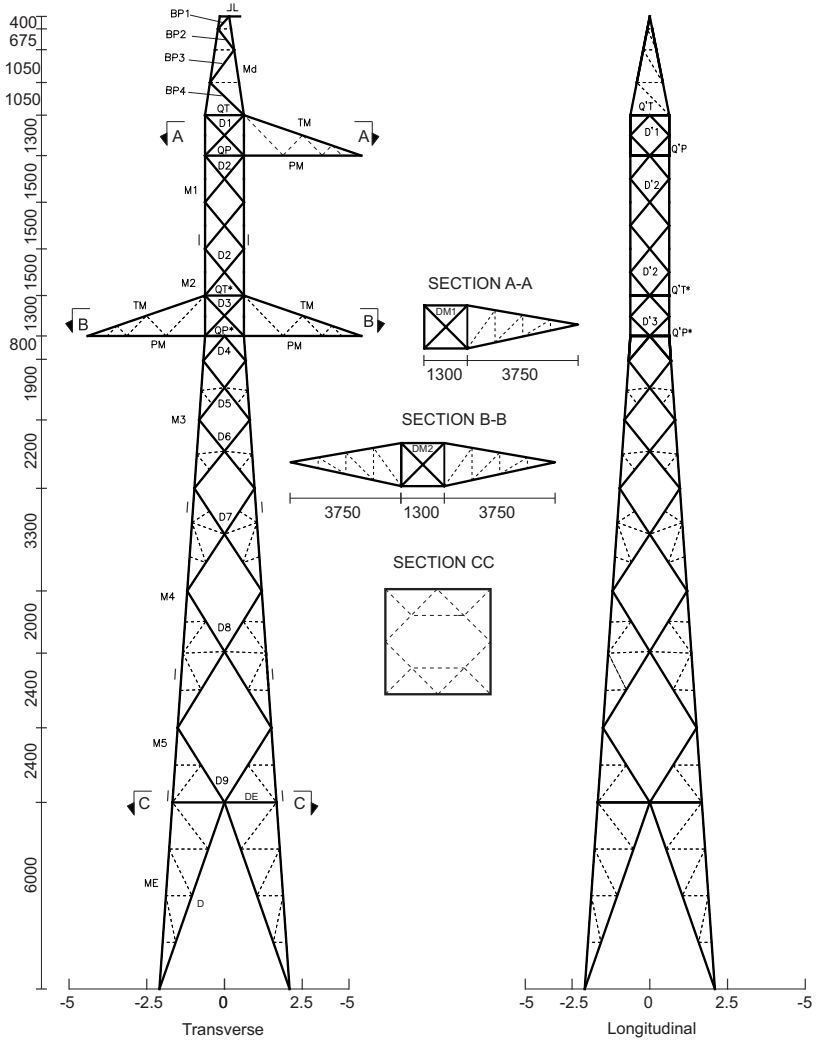

Figure 35 – Electrical clearances.

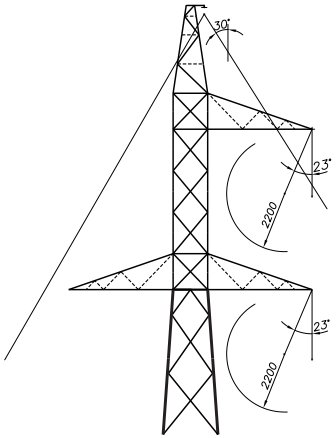

Table 9 – Available profiles for the optimization procedure of the 230 kV transmission tower

Profile (mm)	Area (cm^2)
L 40 × 40 × 3	2.35
L 45 × 45 × 3	2.66
L 50 × 50 × 3	2.96
L 50 × 50 × 4	3.89
L 60 × 60 × 4	4.71
L 60 × 60 × 5	5.82
L 65 × 65 × 4	5.13
L 75 × 75 × 5	7.36
L 75 × 75 × 6	8.75
L 90 × 90 × 6	10.6

The support was subjected to four different load cases, as presented in Figure 36. The first (a) is a yawed wind (75° with the TL axis) load hypothesis, which consists of the wind loads transmitted by the conductors and insulators as well as the wind loads acting on the support itself. The second (b) represents a construction or maintenance

load scenario, presenting horizontal, transversal and vertical components in cross-arms. The third (c) considers a cable conductor rupture, which is combined with a reduced 90° wind load acting on TL. The last (d) considers the ground wire rupture combined with a reduced orthogonal wind acting on TL. Finally, an overload shown in Figure 36 is considered for all cases.

Figure 36 – Load cases for the 230kV tower.

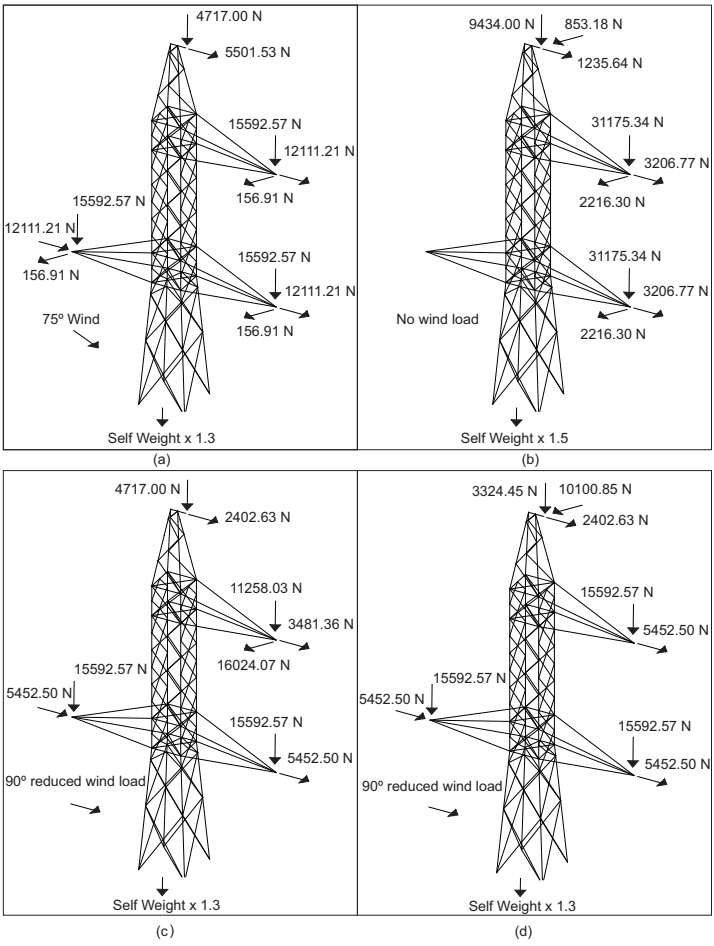

The iterative process to evaluate the wind load in each iteration was also employed to this example. Thus, the wind pressure is determined following the recommendations of IEC (2003), considering a dynamic reference wind pressure of 409 N/m^2 and the terrain roughness of category B. For load cases (c) and (d), the reduced wind load is determined by multiplying the dynamic reference wind pressure by a coefficient equal to 0.36.

The structural analysis was once again performed through an in-house FEM routine developed in MATLAB. Figure 37 presents the final model, in which the truss elements are represented in blue while the frame elements (main legs and diaphragms) are represented in red.

Figure 37 – Final model for the 230kV tower.

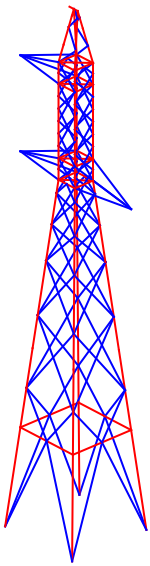

Once again, to understand the influence of the optimization procedure in the final result, three separated studies were performed: i) size optimization; ii) size and shape optimization; iii) size, shape

and topology optimization. Then, to assess each optimization level in the tower weigh reduction the results provided in (ii) and (iii) will be compared to that obtained in (i) and not to the original structure weigh.

In all scenarios the BSA was employed. The BSA parameters were set as: $m_r = 1$, Population size $t_{top} = 30$ and number of cycles $C = 6000$, resulting in 180000 OFE, as in the previous example.

5.2.1 Size optimization

For this example, the bars are grouped as shown in Figure 34. Thus, there are thirty-eight size variables, stored in the design vector $\mathbf{x} = \{a_1, \ldots, a_{38}\}$. Where, a_i is the cross-sectional area of each group. Ten angle profiles with cross-sectional area presented in Table 9 are available for each design variable.

The results are presented in Table 10. The best result found was 2324.7 kg, since all 25 independent runs resulted in identical weights, the average value was 2324.7 kg with a standard deviation of 0.00 kg. A typical convergence history for this case is presented in Figure 38.

As in the previous example of the Section 5.1.1, a detailed analysis of the ratio between the elements internal forces and their capacities confirmed that the optimization led the cross-sectional areas of the bars to their lowest admissible angle profiles. Then, this optimal result will be taken as the reference value to assess the weight reduction obtained with the former results.

Figure 38 – Typical convergence history for the size optimization of the original design.

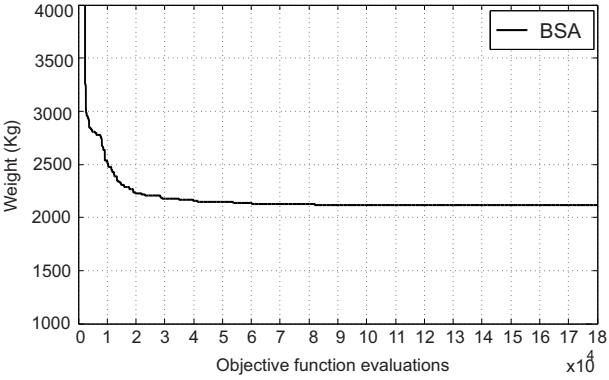

Table 10 – Optimal results for the size optimization of the original structure

GROUP	Area(cm^2)	GROUP	Area(cm^2)
ME	10.6	D'1	2.35
M5	7.36	BP4	2.66
M4	7.36	BP3	2.35
M3	7.36	BP2	2.35
M2	5.82	BP1	2.35
M1	4.71	PM	3.89
Md	2.35	TM	7.36
DP	2.66	QT	2.35
D9	4.71	QP	2.66
D8	4.71	QT*	2.35
D7	2.66	QP*	2.66
D6	2.66	Q'T	2.35
D5	2.35	Q'P	2.35
D4	2.35	Q'T*	2.35
D3	2.66	Q'P'	2.35
D2	2.35	DE	17.5
D1	2.66	DM1	4.71
D'3	2.35	DM2	2.35
D'2	2.66		
Total weight (kg)	2324.7		
Average* (kg)	2324.7		
S.D.* (kg)	0		
Reduction (%)	-		

*Statistical results for 25 runs.

5.2.2 Size and shape optimzation

On this case, the tower shape optimization is performed simultaneously to the size optimization. Figure 39 presents the shape variation scheme. Variation 1 (stored in the design vector as ξ_1) allows the tower base to move horizontally. Variation 2 (stored in the design vector as ξ_2 to ξ_6) allows the nodes of the inclined tower body to move vertically. Variation 3 (stored in the design vector as ξ_7) allows the nodes of the straight tower body to move horizontally. The design vector is now $\mathbf{x} = \{a_1, \ldots, a_{38}, \xi_1, \xi_2, \xi_3, \xi_4, \xi_5, \xi_6, \xi_7\}$. The upper and lower bounds for the variables ξ_1, ξ_2 to ξ_6, and ξ_7 are $[-0.50, 0.50](cm)$, $[-0.30, 0.30](cm)$, and $[-0.20, 0.20](cm)$, respectively. In order to achieve a more practical result the shape variables are allowed to assume discrete values, rounded into centimeters. The bounds for Var. 1 and Var. 3 were decided based on the electrical clearances, while the bounds for the Var. 2 were decided in order to allow a significant shape variation and prevent the layers to overlap.

The results for the size and shape optimization of the original design are presented in Table 11. The best result found has 2138.1 kg, with an average value of 2139.0 kg and standard deviation of 4.40kg. This procedure was able to achieve 8.0% of weight reduction, when compared with the size optimization. Similar to the previous example, the inclusion of the shape optimization provided a significant improvement on the results. A typical convergence curve is presented in Figure 40.

Figure 39 – Shape variation scheme for the 230kV example.

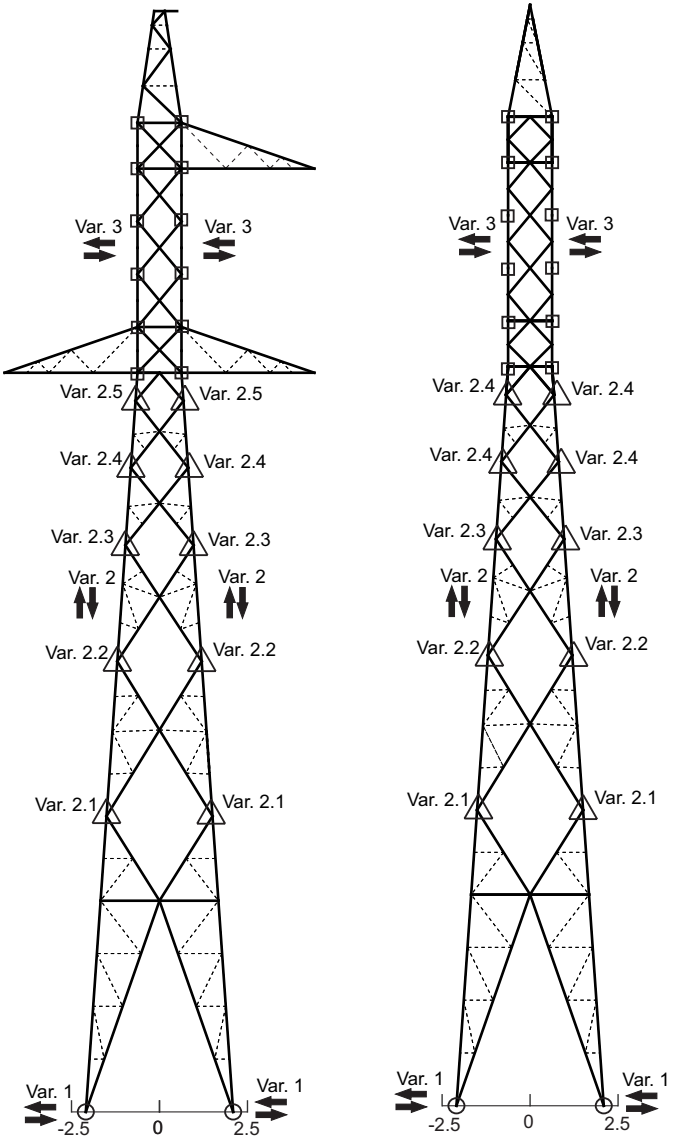

Table 11 – Optimal results for size and shape optimization of the original design

GROUP	Area(cm^2)	GROUP	Area(cm^2)	SHAPE VAR.	Var. (m)
ME	10.6	D'1	2.35	Var. 1	-0.5
M5	8.75	BP4	2.35	Var. 2.1	0.23
M4	7.36	BP3	2.35	Var. 2.2	0.08
M3	7.36	BP2	2.35	Var. 2.3	0.01
M2	7.36	BP1	2.35	Var. 2.4	0.25
M1	4.71	PM	3.89	Var. 2.5	0.06
Md	2.66	TM	7.36	Var. 3	-0.13
DP	2.96	QT	2.35		
D9	2.96	QP	2.66		
D8	2.96	QT*	2.35		
D7	2.66	QP*	2.35		
D6	2.66	Q'T	2.35		
D5	2.35	Q'P	2.35		
D4	2.35	Q'T*	2.35		
D3	2.96	Q'P'	2.35		
D2	2.66	DE	17.5		
D1	2.66	DM1	2.66		
D'3	2.66	DM2	2.35		
D'2	2.66				
Total weight (kg)	2138.1				
Average* (kg)	2139.0				
S.D.* (kg)	4.40				
Reduction (%)	8.0%				

*Statistical results for 25 runs.

Figure 40 – Typical convergence history for the size and shape optimization of the original desing.

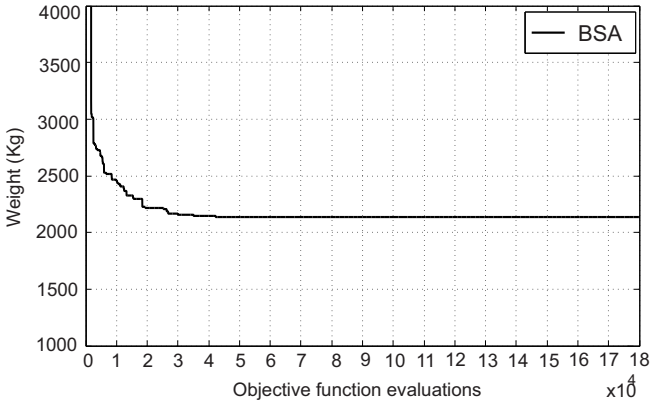

5.2.3 Size, shape and topology optimization

The topological optimization is applied only to the inclined tower body. To perform an independent procedure of the original design, the starting point and the bounds of the geometrical choices (stages 1, 2, 3, and 4 on Figure 17) were defined based on the electrical clearance's requirements and by the usual industrial practice experience (the slope, the angle, and the lengths of the inferior and superior edges *i.e.* and *s.e.*). Then, the parameters α, *i.e.*, *s.e.* and θ are established as 4^{o}, 2.0 meters, 0.5 meters and 90^{o}. The inclined tower body is fixed as 15 meters to attain the sag of the conductors between structures.

In **stage 1** both continuous and staggered bracing pattern were chosen. Then, the design variable τ_1 can assume values $\{0, 1\}$ being 0 for continuous or 1 for staggered bracing. In **stage 2**, 4 possibilities of inferior and superior edges were provided to the staggered bracing tower. Therefore, the design variables τ_2 and τ_3 can assume values $\{1, 2, 3, 4\}$. The continuous bracing tower has 2 possibilities of inferior and superior edges. Then, the design variable τ_2 and τ_3 assume values $\{1, 2\}$. Detailed description is presented in 41.

Figure 41 – Edges for continuous and staggered bracing for the 230kV tower.

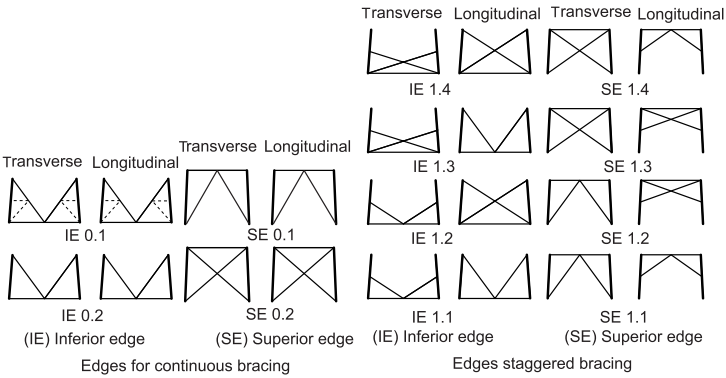

Finally, in **Stage 3**, the proposed methodology is applied to determine the number of internal layers to be furnished for the optimization process. Considering the geometrical values α, *i.e.*, *s.e.* and θ previously defined (4°, 2.0 m, 0.5 m and 90°), the number of calculated layers for continuous bracing tower was 6. Then, the options with 5 and 7 were also provided, i.e., the design variable τ_4 can assume values $\{5, 6, 7\}$. The regression curve illustrated in Figure 19 was employed to define the starting point of the tower body vertical nodes coordinates. For the staggered bracing, an interval with one more layer was provided, i.e., the design variable τ_4 can assume values $\{6, 7, 8\}$. This choice was justified to keep buckling lengths of the tower legs in the same order of magnitude. To determine the vertical coordinates of the internal nodes, the appropriate regression equation for this case was used, which is presented on Figure 20. Consequently, there are 60 possible topologies for the optimization process.

Furthermore, the configuration of the redundant members was kept unchanged. Thus, each one of the 3 internal layers possibilities given for the continuous bracing tower has a fixed redundant member configuration. This procedure is illustrated in Figure 43. An overview of the templates creation procedure, is provided in the flowchart on Figure 42.

The optimal results are presented in Table 12, while the convergence history for a typical run for size, shape and topology optimization is shown in Figure 44. The best result found was 2041.7 kg, the average result for 25 runs was 2105.3 kg and the standard deviation was 22.23 kg. Similar to the previous example, one can notice a higher standard deviation and a similar average value, compared to the size and shape optimization case.

It is important to highlight that the best topology obtained corresponds again to a structure with staggered bracing. In addition, it was possible to find 12.2% of weight reduction, when compared to only size optimization. The design related to the best result is presented on Figure 45.

Figure 42 – Creation of templates for the 230kV tower.

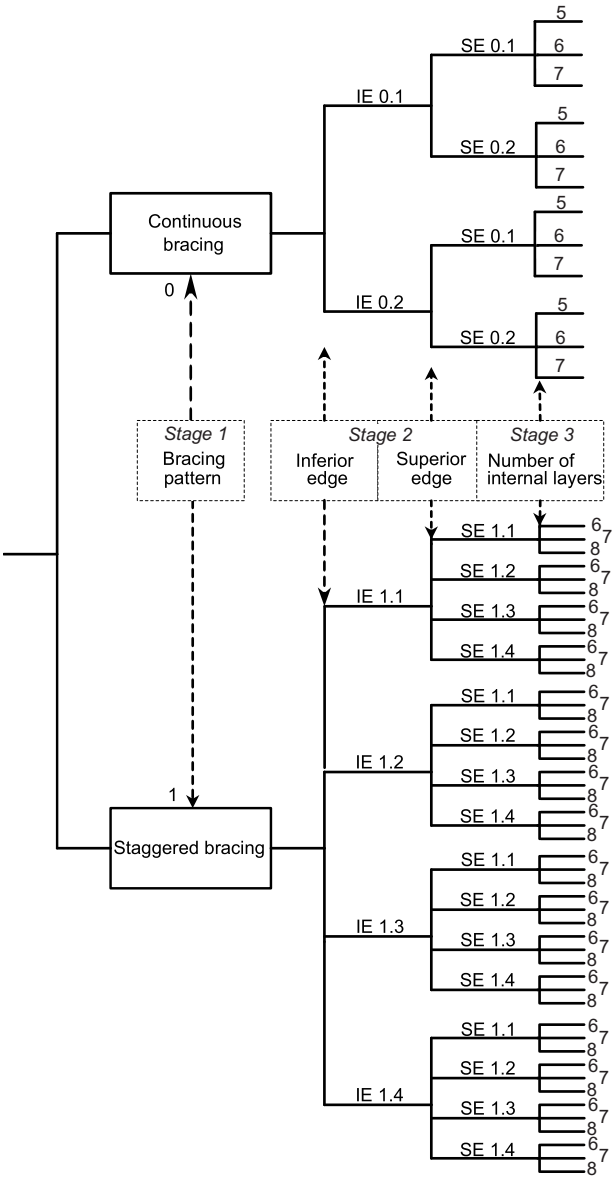

Figure 43 – Variation of internal layers number for the 230kV tower.

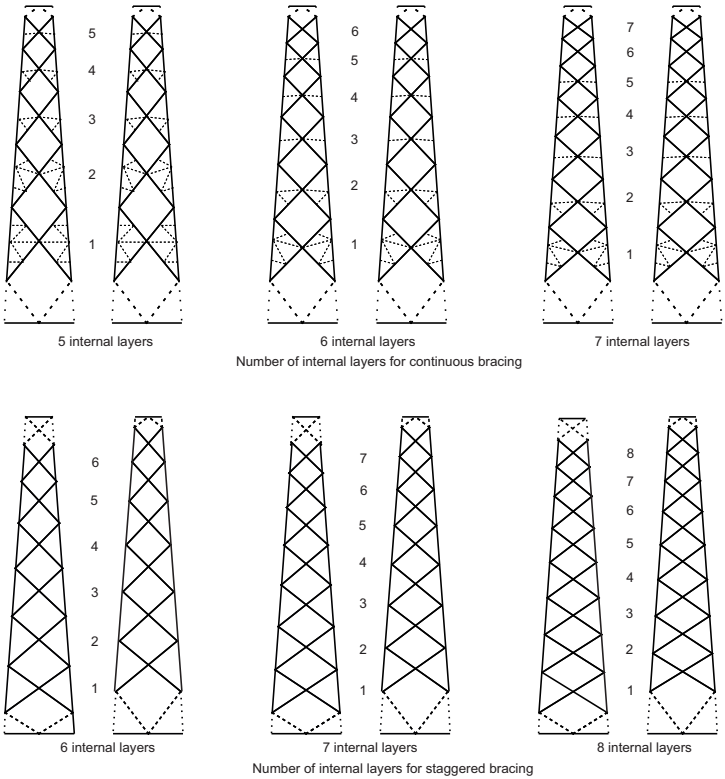

A final test was conducted to assess the optimum size, shape and topology design considering only structures with continuous bracing. Figure 46 presents the best result found, which was 2100.41 kg and corresponds to a structure with three more internal layer than the original topology. Once again, this illustrates the capability of the optimization scheme to create and offer economical topology solutions, once it found two better topologies than the original design. In addition, they are both in accordance with constructional requirements and prototype testing.

Figure 44 – Typical convergence history for the size, shape and topology optimization.

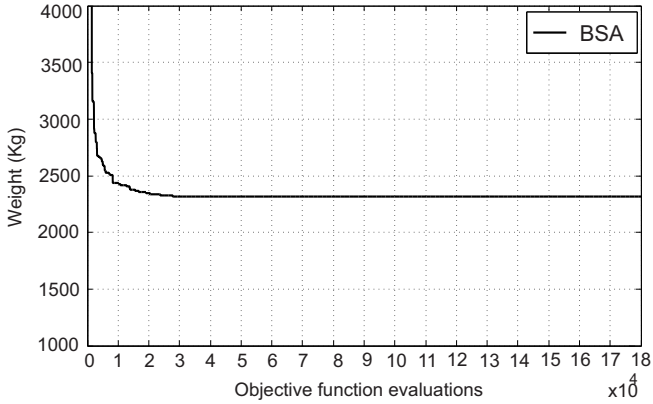

Table 12 – Results for the size, shape and topology optimization

GROUP	Area(cm^2)	GROUP	Area(cm^2)	SHAPE VAR.	Var. (m)
ME	10.6	D'1	2.35	Var. 1	-0.13
M5	10.6	BP4	2.35	Var. 2.1	0.3
M4	8.75	BP3	2.35	Var. 2.2	0.28
M3	7.36	BP2	2.35	Var. 2.3	0.22
M2	7.36	BP1	2.35	Var. 2.4	0.3
M1	4.71	PM	3.89	Var. 2.5	0.12
Md	2.66	TM	7.36	Var. 2.6	0.3
DP	2.96	QT	2.35	Var. 2.7	0.14
D9	2.96	QP	2.35	Var. 2.8	0.3
D8	2.66	QT*	2.35	Var. 2.9	0.2
D7	2.66	QP*	2.35	Var. 2.10	0.2
D6	2.35	Q'T	2.35	Var. 2.11	0.02
D5	2.35	Q'P	2.35	Var. 2.12	0.2
D4	2.35	Q'T*	2.35	Var. 2.13	0.09
D3	2.96	Q'P'	2.35	Var. 2.14	0.2
D2	2.66	DE	17.5	Var. 2.15	0.2
D1	2.66	DM1	2.35	Var. 2.16	0.2
D'3	2.35	DM2	2.35	Var. 2.17	0.2
D'2	2.66			Var. 2.18	0.11
				Var. 3	-0.1
				TOPOLOGY VAR.	
				τ_1	1
Total					
weight (kg)	2041.7			τ_2	2
Average* (kg)	2105.3			τ_3	4
S.D.* (kg)	22.23			τ_4	8
Reduction (%)	12.2%				

*Statistical results for 25 runs.

Figure 45 – Best result found for the proposed approach size, shape and topology optimization.

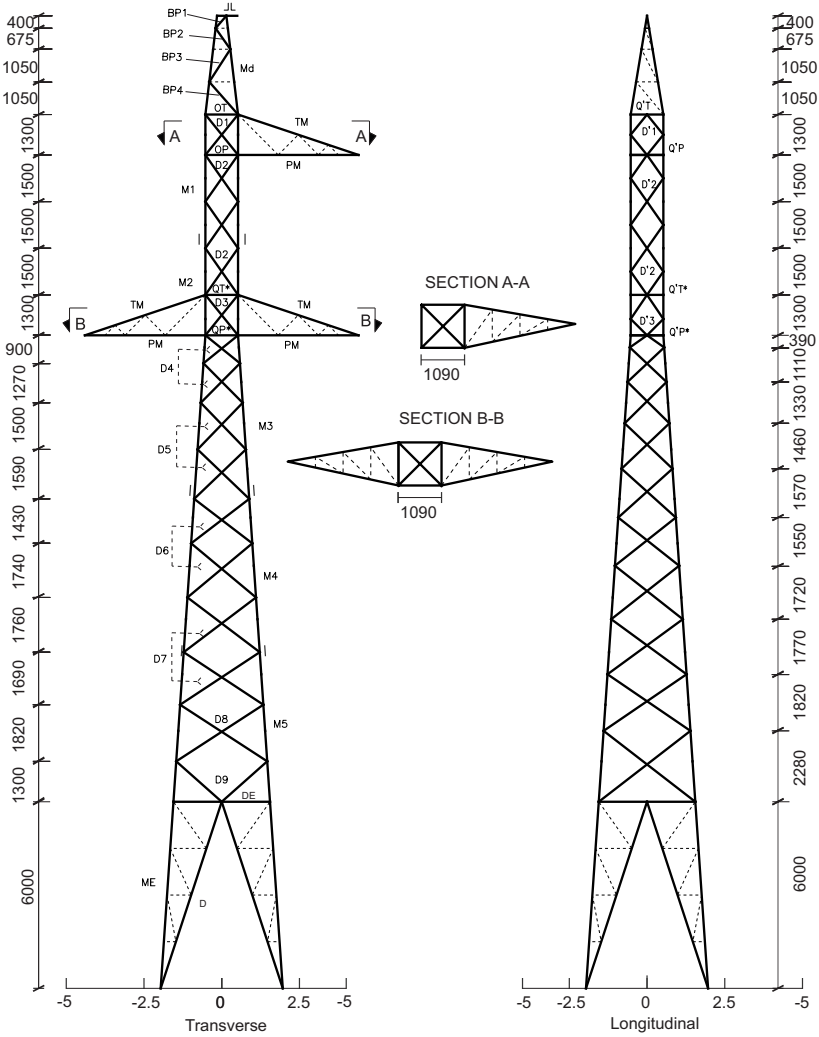

Figure 46 – Best result found for the proposed approach size, shape and topology optimization considering only continuous bracing.

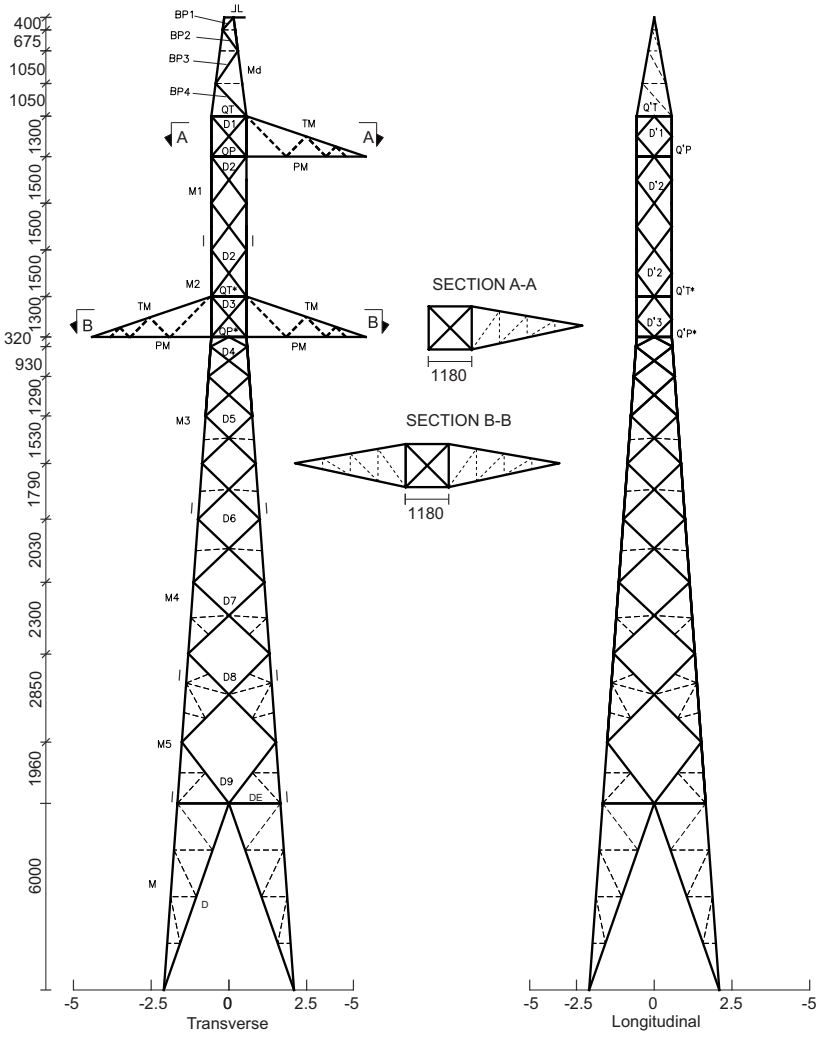

Table 13 – Best results for the three cases studied of 230 kV example

Optimization	Weight (kg)	% reduction
Size	2324.7	-
Size and shape	2138.1	8.0%
Size, shape and topology	2041.7	12.2%

Since this example is subjected to four load cases, instead of two as in Section 5.1, the optimization required around 10h of computational time, using the same hardware configuration (Intel Core i7 3.5GHz with 8 GB of RAM). Finally, the best results for the three cases studied on this example are presented in Table 13.

6 Concluding remarks and future studies

6.1 Concluding remarks

This thesis presented a general methodology for the size, shape and topology optimization of transmission line towers. Two examples were assessed. The first one is a single circuit, self-supported 115kV TLT subjected to a cable conductor rupture scenario and a wind load hypothesis. The second one is a heavier single circuit, self-supported 230kV TLT, subjected to four load cases, including: (i) an yawed wind load hypothesis, (ii) a construction or maintenance load scenario, (iii) a cable conductor rupture hypothesis and (iv) a ground wire rupture scenario. In both examples the constraints from the ASCE 10-15 (2015) were applied.

In this approach, the structure tower is divided in main modules, which can assume different pre- established topologies (templates). A general rule for the templates creation was presented, which is not only based in terms of the design practice, but also in the feasibility of prototype testing. Thus, the optimal solutions reached here are much closer to a direct industrial application than solutions obtained with other existing approaches.

Moreover, in this approach it is not necessary the inclusion of the redundant members in the structural model. Hence, only the correct buckling lengths are declared, which makes the model simpler and easier to work, reducing the possibilities of numerical instabilities.

In particular, the proposed approach is able to handle staggered bracing without difficulties. In fact, the best optimal topology obtained in both studied examples was composed by staggered bracing. This is an important aspect since this structural solution is very usual in practice and it was not addressed in the works found in the literature.

Additionally, in both examples, the proposed scheme was able to reduce up to 12% of the structural weight in comparison to a classical size optimization procedure.

Furthermore, the results presented herein can be used as benchmarks for comparisons in future studies.

6.2 Future studies

Despite the results obtained herein sounds promising, a couple of further efforts must be carried out. Among them:

- The total cost (including, for instance, the fabrication, transportation and assembly) can be used as objective function, instead of only the structural mass.
- Other different self-supporting TLT examples should be performed to assess the optimum topology solutions provided by the proposed procedure. This would allow the establishment of structural patterns, which could be used as a reference for design engineers;
- The verification of the bolts could be included in the dimensioning procedure. Because it impacts on the tension resistance of the elements, an iterative procedure (similar to the one used to determine the wind load) should be applied;
- The procedure could be applied to TLT with pronounced geometrical nonlinear behavior, such as the guyed structures;
- The nonlinear bolt slippage could be also introduced in the modeling, because its influence on the internal member forces distribution is considerable. Then, a more representative structural behavior would be employed.
- The optimum solutions could be numerically assessed until their collapse, aiming to represent a prototype testing. In this case, a more refined structural model with all the nonlinear effects should

be considered. Moreover, a probabilistic assessment should be performed.

References

ADELI, H.; KAMAL, O. Efficient optimization of plane trusses. *Advances in Engineering Software and Workstations*, v. 13, n. 3, p. 116 – 122, 1991. ISSN 0961-3552.

AHMED, K. I. Finite element modeling of non-linear structural response of transmission towers including bolted joint slippage. University of British Columbia, 2007.

AL-BERMANI, F.; KITIPORNCHAI, S. Nonlinear finite element analysis of latticed transmission towers. *Engineering Structures*, Elsevier, v. 15, n. 4, p. 259–269, 1993.

AL-BERMANI, F. G.; KITIPORNCHAI, S. Nonlinear analysis of thin-walled structures using least element/member. *Journal of structural engineering*, American Society of Civil Engineers, v. 116, n. 1, p. 215–234, 1990.

AMERICAN INSTITUTE OF STEEL CONSTRUCTION. *AISC 325-01*: Lrfd manual of steel construction. ., 2001.

AMERICAN SOCIETY OF CIVIL ENGINEERS. *ASCE 10:15*: Design of latticed steel transmission towers. ., 2015.

ARGENTA, M. A. Análise de torres de transmissão submetidas a cargas dinâmicas. Florianópolis, SC, ., 2007.

ARORA, J. *Introduction to optimum design*. .: Academic Press, 2004.

ASSOCIAÇÃO BRASILEIRA DE NORMAS TÉCNICAS. *NBR 6123*: Forças devidas ao vento em edificações. Rio de Janeiro, 1988.

AZEVEDO, C.; DINIZ, S. Towards life-cycle assessment of foundations of guyed towers in electrical transmission lines. In: *First International Symposium on Life-cycle Civil Engineering*. .: ., 2008.

AZEVEDO, C.; DINIZ, S. Probabilistic description of foundation capacity for design of electrical transmission lines. In: *3rd International Symposium on Life-Cycle Civil Engineering*. .: ., 2012.

AZEVEDO, C. P. B. Avaliação da confiabilidade de fundações de torres estaiadas em linhas de transmissão. UFMG, 2007.

AZEVEDO, C. P. B. Projeto de fundações de linhas de transmissão baseado em confiabilidade. UFMG, 2011.

BATTISTA, R.; PFEIL, M. Double controller of wind induced oscillations in telecom towers. In: *International Seminar on Modeling and Identification of Structures Subjected to Dynamic Excitation. Emphasis to Transmission Lines.* .: ., 2009.

BATTISTA, R. C.; RODRIGUES, R. S.; PFEIL, M. S. Dynamic behavior and stability of transmission line towers under wind forces. *Journal of Wind Engineering and Industrial Aerodynamics*, Elsevier, ., v. 91, n. 8, p. 1051–1067, 2003.

CAMP, C.; FARSHCHIN, M. Design of space trusses using modified teaching–learning based optimization. *Engineering Structures*, v. 62–63, p. 87 – 97, 2014. ISSN 0141-0296.

CARVALHO, H. *Metodologias para análise estática do efeito do vento em linhas de transmissão*. Tese (Doutorado) — Tese de Doutorado. Universidade Federal de Minas Gerais. Minas Gerais, 2010.

CARVALHO, H. *Avaliação dos Efeitos de Vento em Linhas de Transmissão*. Tese (Doutorado) — Tese de Doutorado. Universidade Federal de Minas Gerais. Minas Gerais, 2015.

CHEN, J.; YUAN, F.; JIANG, L. Optimal design of transmission line tower based intelligent selection. In: *Proceedings of The Canadian Society for Mechanical Engineering International Congress.* .: ., 2014.

CIVICIOGLU, P. Backtracking search optimization algorithm for numerical optimization problems. *Applied Mathematics and Computation*, Elsevier, v. 219, n. 15, p. 8121–8144, 2013.

CONCEIçãO, R. S. *Torres de Transmissão Sob Ação de Ventos Originados de Ciclones Extratropicais e de Downbursts*. Tese (Doutorado) — Universidade Federal do Rio de Janeiro, 2013.

CONSEIL INTERNATIONAL DES GRANDS RéSEAUX ELECTRIQUES. *CIGRÉ Brochure 138*: An experiment to measure the variation in lattice tower strength due to local design practice. Paris, 1991.

CONSEIL INTERNATIONAL DES GRANDS RéSEAUX ELECTRIQUES. *CIGRÉ Brochure 387*: Influence of the hyperstatic modeling on the behavior of transmission line lattice structures. Paris, 2009.

COSTA, R. S. *Formulação para a análise avançada de sistemas estruturais formados por cabos e treliças espaciais visando à aplicação em torres estaiadas para linhas de transmissão*. Tese (Doutorado) — Tese de doutorado. Universidade Federal de Minas Gerais. Minas Gerais, 2014.

DOBBS, M. W.; FELTON, L. P. Optimization of truss geometry. *Journal of the Structural Division*, ASCE, v. 95, n. 10, p. 2105–2118, 1969.

DOMINGUEZ, A.; STIHARU, I.; SEDAGHATI, R. Practical design optimization of truss structures using the genetic algorithms. *Research in Engineering Design*, Springer, v. 17, n. 2, p. 73–84, 2006.

DORN, W. S. Automatic design of optimal structures. *Journal de mecanique*, v. 3, p. 25–52, 1964.

FANG, S.-j.; ROY, S.; KRAMER, J. Transmission structures. *In: Ed. Chen Wai-Fah, Structural engineering handbook*, CRC Press LLC, Boca Raton, Fla, USA, 1999.

FINOTTO, V.; SILVA, W. D.; VALÁŠEK, M.; ŠTEMBERK, P. Hybrid fuzzy-genetic system for optimising cabled-truss structures. *Advances in Engineering Software*, Elsevier, v. 62, p. 85–96, 2013.

GABRIELLI, T. V. *Analise do Comportamento Estrutural de Torres de Transmissão Tubulares via Simulação Computacional*. Tese (Doutorado) — Universidade Federal de Ouro Preto, 2004.

GALANTE, M. Genetic algorithms as an approach to optimize real-world trusses. *International Journal for Numerical Methods in Engineering*, Wiley Online Library, v. 39, n. 3, p. 361–382, 1996.

GOLDBERG, D. E.; SAMTANI, M. P. Engineering optimization via genetic algorithm. In: ASCE. *Electronic Computation (1986)*. .: ., 1986. p. 471–482.

GOMES, W. J. de S.; BECK, A. T. Global structural optimization considering expected consequences of failure and using ann surrogates. *Computers & Structures*, Elsevier, v. 126, p. 56–68, 2013.

GONTIJO, C. R. *Contribuição a análise e projeto de torres autoportantes de linhas de transmissão*. Tese (Doutorado) — Dissertação de mestrado. Universidade Federal de Minas Gerais. Minas Gerais, 1994.

GRIERSON, D.; PAK, W. Optimal sizing, geometrical and topological design using a genetic algorithm. *Structural Optimization*, Springer, v. 6, n. 3, p. 151–159, 1993.

GUO, H.; LI, Z. Structural topology optimization of high-voltage transmission tower with discrete variables. *Structural and Multidisciplinary Optimization*, Springer, v. 43, n. 6, p. 851–861, 2011.

HAJELA, P.; LEE, E. Genetic algorithms in truss topological optimization. *International journal of solids and structures*, Elsevier, v. 32, n. 22, p. 3341–3357, 1995.

HEMP, W. S. *Optimum structures*. .: Clarendon Press, 1973.

INTERNATIONAL ELECTROTECHNICAL COMMISSION. *IEC 60826:2003*: Design criteria of overhead transmission lines. ., 2003.

KAMINSKI-JR, J. Incertezas de modelo na análise de torres metálicas treliçadas de linhas de transmissão. 2007.

KAMINSKI-JR., J.; RIERA, J.; MENEZES, R. de; MIGUEL, L. F. Model uncertainty in the assessment of transmission line towers subjected to cable rupture. *Engineering Structures*, v. 30, n. 10, p. 2935 – 2944, 2008.

KAVEH; GHOLIPOUR; RAHAMI. Optimal design of transmission towers using genetic algorithm and neural networks. *International Journal of Space Structures*, Multi Science Publishing, v. 23, n. 1, p. 1–19, 2008.

KELESOGLU, O. Fuzzy multiobjective optimization of truss-structures using genetic algorithm. *Advances in Engineering Software*, Elsevier, v. 38, n. 10, p. 717–721, 2007.

KITIPORNCHAI, S.; AL-BERMANI, F.; PEYROT, A. Effect of bolt slippage on ultimate behavior of lattice structures. *Journal of Structural Engineering*, v. 120, n. 8, p. 2281–2287, 1994.

KROEKER, D. *Structural analysis of transmission towers with connection slip modeling*. Tese (Doutorado) — University of Manitoba, 2000.

LOPEZ, R.; LUERSEN, M.; CURSI, E. Optimization of laminated composites considering different failure criteria. *Composites Part B: Engineering*, Elsevier, v. 40, n. 8, p. 731–740, 2009.

LOPEZ, R. H.; LUERSEN, M. A.; CURSI, J. E. S. d. Optimization of hybrid laminated composites using a genetic algorithm. *Journal of the Brazilian Society of Mechanical Sciences and Engineering*, SciELO Brasil, v. 31, n. 3, p. 269–278, 2009.

LOREDO-SOUZA, A.; DAVENPORT, A. The effects of high winds on transmission lines. *Journal of Wind Engineering and Industrial Aerodynamics*, Elsevier, v. 74, p. 987–994, 1998.

LOREDO-SOUZA, A.; DAVENPORT, A. A novel approach for wind tunnel modelling of transmission lines. *Journal of wind engineering and industrial aerodynamics*, Elsevier, v. 89, n. 11, p. 1017–1029, 2001.

LOREDO-SOUZA, A.; DAVENPORT, A. The influence of the design methodology in the response of transmission towers to wind loading. *Journal of wind engineering and industrial aerodynamics*, Elsevier, v. 91, n. 8, p. 995–1005, 2003.

MARA, T. G. *Capacity Assessment of a Transmission Tower under Wind Loading*. Tese (Doutorado) — University of Western Ontario, 2013.

MATHAKARI, S.; GARDONI, P.; AGARWAL, P.; RAICH, A.; HAUKAAS, T. Reliability-based optimal design of electrical transmission towers using multi-objective genetic algorithms. *Computer-Aided Civil and Infrastructure Engineering*, Wiley Online Library, v. 22, n. 4, p. 282–292, 2007.

MENEZES, R. C. R. d. Estudos de confiabilidade de linhas de transmissão submetidas à ação do vento. 1988.

MEZURA-MONTES, E.; COELLO, C. A. C. Constraint-handling in nature-inspired numerical optimization: past, present and future. *Swarm and Evolutionary Computation*, Elsevier, v. 1, n. 4, p. 173–194, 2011.

MIGUEL, L. F. F.; JR., J. K.; MIGUEL, L. F. F.; RIERA, J. D.; MENEZES, R. C. R. de. Dynamic response of a 190m-high transmission tower for a large river crossing. *Journal of Civil Engineering and Management*, v. 22, n. 4, p. 509–519, 2016.

MIGUEL, L. F. F.; LOPEZ, R. H.; MIGUEL, L. F. F. A hybrid approach for damage detection of structures under operational conditions. *Journal of Sound and Vibration*, Elsevier, v. 332, n. 18, p. 4241–4260, 2013.

MIGUEL, L. F. F.; LOPEZ, R. H.; MIGUEL, L. F. F. Multimodal size, shape, and topology optimisation of truss structures using the firefly

algorithm. *Advances in Engineering Software*, Elsevier, v. 56, p. 23–37, 2013.

MIGUEL, L. F. F.; MIGUEL, L. F. F.; RIERA, J. D.; JR., J. K.; MENEZES, R. C. R. de. Assessment of code recommendations through simulation of {EPS} wind loads along a segment of a transmission line. *Engineering Structures*, v. 43, p. 1 – 11, 2012.

NATARAJAN, K.; SANTHAKUMAR, A. Reliability-based optimization of transmission line towers. *Computers & structures*, Elsevier, v. 55, n. 3, p. 387–403, 1995.

NETO, W. T. D. *Torres de Linhas de Transmissão sob Ação de Ventos Originados de Tormentas Elétricas*. Tese (Doutorado) — Universidade Federal do Rio de Janeiro, 2012.

NHAMAGE, I. A. *et al.* Aperfeiçoamento do algoritmo de otimização híbrido pincus-nelder e mead para detecção de dano em estruturas a partir de dados vibracionais. 2014.

NOCEDAL, J.; WRIGHT, S. *Numerical optimization*. .: Springer Science & Business Media, 2006.

NOILUBLAO, N.; BUREERAT, S. Simultaneous topology, shape and sizing optimisation of a three-dimensional slender truss tower using multiobjective evolutionary algorithms. *Computers & Structures*, Elsevier, v. 89, n. 23, p. 2531–2538, 2011.

OLIVEIRA, M.; SILVA, J. da; ANDRADE, S. de; VELLASCO, P.; LIMA, L. de. Structural analysis of transmission line steel towers subjected to wind induced dynamic actions. In: *Proceedings of The Thirteenth International Conference on Civil, Structural and Environmental Engineering Computing*. .: ., 2003.

OLIVEIRA, M. I. R. d.; SILVA, J. A. G. S. d.; VELLASCO, P. C. G. d. S.; ANDRADE, S. A. A. L. d.; LIMA, L. R. O. d. Structural analysis of guyed steel telecommunication towers for radio antennas. *Journal of the Brazilian Society of Mechanical Sciences and Engineering*, v. 29, p. 185 – 195, 06 2007. ISSN 1678-5878.

OLIVEIRA, M. I. R. de; NISHIO, C.; NEVES, A. da S.; REGO, M. R. de M.; JÚNIOR, C. M. P. Análise estrutural de torres de transmissão de energia submetidas aos efeitos dinâmicos induzidos pelo vento. 2006.

PARIS, J.; MARTINEZ, S.; NAVARRINA, F.; COLOMINAS, I.; CASTELEIRO, M. Structural optimization of high voltage transmission line towers considering continuum and discrete design variables. *Computer Aided Optimum Design in Engineering XII*, WIT Press, v. 125, p. 59, 2012.

PARIS, J.; MARTINEZ, S.; NAVARRINA F COLOMINAS, I.; CASTELEIRO, M. Structural optimization of high tension. In: *2nd International Conference on Engineering Optimization September 6-9.* Lisbon, Portugal: ., 2010.

PEDERSEN, P. On the optimal layout of multi-purpose trusses. *Computers & Structures*, Elsevier, v. 2, n. 5, p. 695–712, 1972.

RABELO, J.; JR, C. C.; GRECO, M. Análise comparativa do peso de uma mísula de torre de linha de transmissão construída em plástico reforçado por fibra de vidro e em aço. In: *Anais do VIII Congresso Nacional de Engenharia Mecânica*. .: ., 2014. .

RAHAMI, H.; KAVEH, A.; GHOLIPOUR, Y. Sizing, geometry and topology optimization of trusses via force method and genetic algorithm. *Engineering Structures*, v. 30, n. 9, p. 2360 – 2369, 2008. ISSN 0141-0296.

RAJAN, S. Sizing, shape, and topology design optimization of trusses using genetic algorithm. *Journal of Structural Engineering*, American Society of Civil Engineers, 1995.

RAJEEV, S.; KRISHNAMOORTHY, C. Discrete optimization of structures using genetic algorithms. *Journal of structural engineering*, American Society of Civil Engineers, 1992.

RIPPEL, L. I. Estudo em túnel de vento do arrasto aerodinâmico sobre torres treliçadas de linhas de transmissão. 2005.

RODRIGUES, R.; BATTISTA, R.; PFEIL, M. A new model for an old problem - the dynamic mechanism of collapse of transmission line towers under wind forces. In: *1st Americas Conference on Wind Engineering*. .: ., 2001.

RODRIGUES, R.; BATTISTA, R.; PFEIL, M. Modelo não-linear dinâmico para a análise de colapso de torres de linhas de transmissão sob ação de vento. In: *XXXI Jornadas Sud- Americanas de Ingeniería Estructural*. .: ., 2004.

RODRIGUES, R.; BATTISTA, R.; PFEIL, M. Atenuação dinâmica de torres de transmissão de energia elétrica sob ação de vento. In: *XXVI Iberian Latin-American Congress on Computational Methods in Engineering*. .: ., 2005.

SAKA, M. Shape optimization of trusses. *Journal of the Structural Division*, ASCE, v. 106, n. 5, p. 1155–1174, 1980.

SHEA, K.; SMITH, I. F. Improving full-scale transmission tower design through topology and shape optimization. *Journal of structural engineering*, American Society of Civil Engineers, v. 132, n. 5, p. 781–790, 2006.

SILVA, J. da; VELLASCO, P.; ANDRADE, S.; OLIVEIRA. The influence of structural steel design models on the behaviour of slender transmission and telecommunication towers. In: *Proceedings of 9th International Conference on Civil and Structural Engineering Computing*. .: ., 2003.

SINGH, K. *Análise estática de torres metálicas autoportantes para linhas de transmissão*. Tese (Doutorado) — Dissertação de Mestrado. Universidade de Brasília. Distrito Federal, 2009.

SIVAKUMAR, P.; RAJARAMAN, A.; KNIGHT, G. S.; RAMACHANDRAMURTHY, D. Object-oriented optimization approach using genetic algorithms for lattice towers. *Journal of computing in civil engineering*, American Society of Civil Engineers, v. 18, n. 2, p. 162–171, 2004.

SOLEIMANI, H.; KANNAN, G. A hybrid particle swarm optimization and genetic algorithm for closed-loop supply chain network design in large-scale networks. *Applied Mathematical Modelling*, Elsevier, v. 39, n. 14, p. 3990–4012, 2015.

SOUZA, R. R. de; MIGUEL, L. F. F.; LOPEZ, R. H.; MIGUEL, L. F. F.; TORII, A. J. A procedure for the size, shape and topology optimization of transmission line tower structures. *Engineering Structures*, Elsevier, v. 111, p. 162–184, 2016.

SVED, G.; GINOS, Z. Structural optimization under multiple loading. *International Journal of Mechanical Sciences*, Elsevier, v. 10, n. 10, p. 803–805, 1968.

TANG, W.; TONG, L.; GU, Y. Improved genetic algorithm for design optimization of truss structures with sizing, shape and topology variables.

International Journal for Numerical Methods in Engineering, Wiley Online Library, v. 62, n. 13, p. 1737–1762, 2005.

TANIWAKI, K.; OHKUBO, S. Optimal synthesis method for transmission tower truss structures subjected to static and seismic loads. *Structural and Multidisciplinary Optimization*, Springer, v. 26, n. 6, p. 441–454, 2004.

TORII, A. J.; LOPEZ, R. H.; BIONDINI, F. An approach to reliability-based shape and topology optimization of truss structures. *Engineering Optimization*, Taylor & Francis, v. 44, n. 1, p. 37–53, 2012.

TORII, A. J.; LOPEZ, R. H.; MIGUEL, L. F. F. Modeling of global and local stability in optimization of truss-like structures using frame elements. *Structural and Multidisciplinary Optimization*, v. 51, n. 6, p. 1187–1198, 2014. ISSN 1615-1488.

UNGKURAPINAN, N.; CHANDRAKEERTHY, S. D. S.; RAJAPAKSE, R.; YUE, S. Joint slip in steel electric transmission towers. *Engineering Structures*, Elsevier, v. 25, n. 6, p. 779–788, 2003.

VELLASCO, P.; SILVA, J. da; ; ANDRADE, S.; OLIVEIRA. An evaluation of structural steel design systems for transmission and telecommunication towers. In: *Proceedings of the International Symposium on Lightweight Structures in Civil Engineering. .*: ., 2002.

WANG, H.; OHMORI, H. Elasto-plastic analysis based truss optimization using genetic algorithm. *Engineering Structures*, Elsevier, v. 50, p. 1–12, 2013.

WU, S.-J.; CHOW, P.-T. Integrated discrete and configuration optimization of trusses using genetic algorithms. *Computers & structures*, Elsevier, v. 55, n. 4, p. 695–702, 1995.

ZHU, K.; AL-BERMANI, F.; KITIPORNCHAI, S. Nonlinear dynamic analysis of lattice structures. *Computers and Structures*, v. 52, n. 1, p. 9–15, 1994.

7 Appendix

7.1 Design methodology

Considering a Load and Resistance Factor Design methodology (LRFD), the following condition must be satisfied:

$$S_d \leq R_d \tag{7.1}$$

Where S_d is the design factored load and R_d is the design factored resistance. S_d is taken directly from the original design, which was properly determined following a probabilistic sense. R_d is determined through the product of the nominal resistance (R_n) by the resistance factor (ϕ_r), as shown in Equation 7.2.

$$R_d = \phi_r \cdot R_n \tag{7.2}$$

The tension and compression nominal resistances (R_n) are determined according to the ASCE 10-15 (2015). The resistance factor ϕ_r is considered equals to 0.93, following the current Brazilian industrial practice.

7.1.1 Compression members

For compression members, R_n is determined following Equation 7.3:

$$R_n = F_a \cdot A_g \tag{7.3}$$

Where A_g is the cross sectional area of the member and F_a is the design compressive stress, determined according to Equation 7.4.

$$\text{if} \quad \frac{KL}{r} \leq C_c \quad \text{, then} \tag{7.4}$$

$$F_a = \left[1 - \frac{1}{2}\left(\frac{KL/r}{C_c}\right)^2\right] F_y$$

$$\text{if} \quad \frac{KL}{r} \leq C_c \quad \text{, then}$$

$$F_a = \frac{\pi^2 E}{\left(\frac{KL}{r}\right)^2}$$

$$\text{Where,} \quad C_c = \pi\sqrt{\frac{2E}{F_y}}$$

In Equation 7.4, F_y is the minimum guaranteed yield stress, E is the modulus of elasticity, L is the unbraced length, r is radius of gyrations and K is effective length coefficient.

The effective length KL depends on the type of connection used in the element. The following options are provided:

- For leg members bolted in both faces at connections.

Equation 1: $\frac{KL}{r} = \frac{L}{r} \quad 0 \leq \frac{L}{r} \leq 150.$

- For members with a concentric load at one end and normal framing eccentricity at the other end of the unsupported panel.

Equation 2: $\frac{KL}{r} = 30 + \frac{L}{r}0.75 \quad 0 \leq \frac{L}{r} \leq 120$

- For members with normal framing eccentricities at both ends of the unsupported panel.

Equation 3: $\frac{KL}{r} = 60 + \frac{L}{r}0.5 \quad 0 \leq \frac{L}{r} \leq 120$

- For members unrestrained against rotation at both ends of the unsupported panel.

Equation 4: $\frac{KL}{r} = \frac{L}{r} \quad 120 \leq \frac{L}{r} \leq 200$

- For members partially restrained against rotation at one end of the unsupported panel.

Equation 5: $\frac{KL}{r} = 28.6 + \frac{L}{r}0.762 \quad 120 \leq \frac{L}{r} \leq 225$

- For members partially restrained against rotation at both ends of the unsupported panel.

Equation 6: $\frac{KL}{r} = 46.2 + \frac{L}{r}0.615 \quad 120 \leq \frac{L}{r} \leq 250$

Because the bolts are not verified in the present work, the effective length KL is determined through the Equation 1 for leg members and the Equation 3 for other members in general.

The local buckling is taking into account verifying the ratio w/t, where w is the flat width and t is the leg thickness.

$$
\begin{aligned}
\text{if } \left(\frac{w}{t}\right) < \left(\frac{w}{t}\right)_{lim} \text{,then} \quad & (7.5)\\
F_{cr} = F_y & \\
\text{if } \left(\frac{w}{t}\right)_{lim} \leq \left(\frac{w}{t}\right) \leq \frac{144 \cdot 2.62}{\sqrt{F_y}} \text{ ,then} & \\
F_{cr} = \left[1.677 - 0.677\frac{w/t}{(w/t)_{lim}}\right] F_y & \\
\text{if } \left(\frac{w}{t}\right) > \frac{144 \cdot 2.62}{\sqrt{F_y}} \text{ ,then} & \\
F_{cr} = \frac{0.0332\pi^2 E}{(w/t)^2} & \\
\text{Where, } \left(\frac{w}{t}\right)_{lim} = \frac{80 \cdot 2.62}{\sqrt{F_y}} &
\end{aligned}
$$

Therefore, the design compression stress Fa of Equation 7.4 must be determined replacing the value of Fy by the Fcr furnished in Equation 7.5. Angles with w/t superior than 25 are not allowed.

7.1.2 Tension members

For tensioned members, R_n is determined following Equation 7.6.

$$R_n = A_n \cdot F_t \tag{7.6}$$

F_t is divided in two groups:

- for concentrically loaded tensioned members:
  $F_t = F_y$
- for angles connected by one leg:
  $F_t = 0.9 \cdot F_y$

The net cross sectional area (A_n) is the gross cross sectional area minus the loss due holes. To compute this loss, the diameter of the bolt

hole that has been punched shall be taken as 1.6 millimeters greater than the nominal diameter of the hole.

The connection resistance was not verified in this study. However, to take into account the bolt presence in the evaluation of the net area, the gross area is reduced by considering the presence of two 12mm bolts for leg members and one 12mm bolt for other members in general.

7.1.3 Slenderness ratios

The maximum values for slenderness ratio are set as: 150 for compressed leg members, 250 for other compressed members and 300 for tensioned members.